NAVAL POSTGRADUATE SCHOOL

MONTEREY, CALIFORNIA

THESIS

USING RADIO OCCULTATIONS TO ASSESS THE UNCERTAINTY OF MOISTURE IN THE TROPICAL TROPOSPHERE

by

Michael Adamski Jr.

December 2021

Thesis Advisor: John M. Peters
Second Reader: Scott Powell

THIS PAGE INTENTIONALLY LEFT BLANK

REPORT DOCUMENTATION PAGE	*Form Approved OMB No. 0704-0188*

1. AGENCY USE ONLY *(Leave blank)*	**2. REPORT DATE** December 2021	**3. REPORT TYPE AND DATES COVERED** Master's thesis

4. TITLE AND SUBTITLE
USING RADIO OCCULTATIONS TO ASSESS THE UNCERTAINTY OF MOISTURE IN THE TROPICAL TROPOSPHERE

5. FUNDING NUMBERS

6. AUTHOR(S) Michael Adamski Jr.

7. PERFORMING ORGANIZATION NAME(S) AND ADDRESS(ES)
Naval Postgraduate School
Monterey, CA 93943-5000

8. PERFORMING ORGANIZATION REPORT NUMBER

9. SPONSORING / MONITORING AGENCY NAME(S) AND ADDRESS(ES)
N/A

10. SPONSORING / MONITORING AGENCY REPORT NUMBER

11. SUPPLEMENTARY NOTES The views expressed in this thesis are those of the author and do not reflect the official policy or position of the Department of Defense or the U.S. Government.

12a. DISTRIBUTION / AVAILABILITY STATEMENT
Approved for public release. Distribution is unlimited.

12b. DISTRIBUTION CODE
A

13. ABSTRACT (maximum 200 words)

Global Navigation Satellite Systems (GNSS) satellites are constantly orbiting the Earth in a Medium Earth Orbit (MEO) at an altitude of approximately 20,200 km. GNSS satellites in MEO continuously direct signals towards Earth for terrestrial users, but some signals are bent or refracted back into space. Low Earth Orbiting (LEO) satellites equipped with the proper equipment can receive these radio occultations (RO) and transmit them to ground stations for processing and dissemination. RO data produces profiles or atmospheric soundings of water vapor, temperature, and pressure. This research uses RO profiles to expose the uncertainty of moisture in the tropical troposphere. The tropical troposphere's moisture uncertainty is critical for determining if convection occurs and assessing updraft strength and buoyancy in the planetary boundary layer to determine intensity. Moisture uncertainty above the planetary boundary layer impacts how detrimental entrainment can be for the generation of thunderstorms. Cloud Model 1 (CM1) numerical simulations demonstrate how moisture uncertainty will affect thunderstorm forecasts. Quantifying uncertainty in the tropical troposphere and demonstrating its effects is critical for improving forecasts in the tropics, where the Navy is commonly operating.

14. SUBJECT TERMS
radio occultation, relative humidity, entrainment, moisture uncertainty, tropical troposphere, thunderstorms, Global Navigation Satellite Systems, GNSS, Medium Earth Orbit, MEO, Low Earth Orbit, LEO, radio occultations, RO, Cloud Model 1, CM1

15. NUMBER OF PAGES
77

16. PRICE CODE

17. SECURITY CLASSIFICATION OF REPORT	**18. SECURITY CLASSIFICATION OF THIS PAGE**	**19. SECURITY CLASSIFICATION OF ABSTRACT**	**20. LIMITATION OF ABSTRACT**
Unclassified	Unclassified	Unclassified	UU

NSN 7540-01-280-5500

Standard Form 298 (Rev. 2-89)
Prescribed by ANSI Std. 239-18

THIS PAGE INTENTIONALLY LEFT BLANK

Approved for public release. Distribution is unlimited.

USING RADIO OCCULTATIONS TO ASSESS THE UNCERTAINTY OF MOISTURE IN THE TROPICAL TROPOSPHERE

Michael Adamski
Lieutenant Commander, United States Navy
BS, United States Naval Academy, 2011

Submitted in partial fulfillment of the
requirements for the degree of

MASTER OF SCIENCE IN METEOROLOGY AND PHYSICAL OCEANOGRAPHY

from the

NAVAL POSTGRADUATE SCHOOL
December 2021

Approved by: John M. Peters
Advisor

Scott Powell
Second Reader

Wendell A. Nuss
Chair, Department of Meteorology

THIS PAGE INTENTIONALLY LEFT BLANK

ABSTRACT

Global Navigation Satellite Systems (GNSS) satellites are constantly orbiting the Earth in a Medium Earth Orbit (MEO) at an altitude of approximately 20,200 km. GNSS satellites in MEO continuously direct signals towards Earth for terrestrial users, but some signals are bent or refracted back into space. Low Earth Orbiting (LEO) satellites equipped with the proper equipment can receive these radio occultations (RO) and transmit them to ground stations for processing and dissemination. RO data produces profiles or atmospheric soundings of water vapor, temperature, and pressure. This research uses RO profiles to expose the uncertainty of moisture in the tropical troposphere. The tropical troposphere's moisture uncertainty is critical for determining if convection occurs and assessing updraft strength and buoyancy in the planetary boundary layer to determine intensity. Moisture uncertainty above the planetary boundary layer impacts how detrimental entrainment can be for the generation of thunderstorms. Cloud Model 1 (CM1) numerical simulations demonstrate how moisture uncertainty will affect thunderstorm forecasts. Quantifying uncertainty in the tropical troposphere and demonstrating its effects is critical for improving forecasts in the tropics, where the Navy is commonly operating.

THIS PAGE INTENTIONALLY LEFT BLANK

TABLE OF CONTENTS

THIS PAGE INTENTIONALLY LEFT BLANK

LIST OF FIGURES

THIS PAGE INTENTIONALLY LEFT BLANK

LIST OF TABLES

THIS PAGE INTENTIONALLY LEFT BLANK

LIST OF ACRONYMS AND ABBREVIATIONS

AMIP	Atmospheric Model Intercomparison Project
AMS	American Meteorological Society
AOI	Area of Interest
CAPE	Convective Available Potential Energy
CDAAC	COSMIC Data Analysis and Archive Center
CFSR	Climate Forecast System Reanalysis
CI	Confidence Intervals
COSMIC	Constellation Observing System for Meteorology, Ionosphere, and Climate
CM1	Cloud Model-1
DOD	Department of Defense
DOE	Department of Energy
ECMWF	European Centre for Medium-Range (ECMWF) Weather Forecasts
ERA5	ECMWF Reanalysis 5
ESRL	Earth System Research Laboratories
GCC	Geographic Combatant Commands
GNSS	Global Navigation Satellite Systems
GU	Guam
INDOPACOM	Indo-Pacific Command
LEO	Low Earth Orbit
NAVGEM	Navy Global Environmental Model
NCEP	National Center for Environmental Prediction
NOAA	National Oceanographic Atmospheric Administration
NORM	Normalized
NWS	National Weather Service
NWSO	National Weather Service Office
MAD	Mean Absolute Difference
MEO	Medium Earth Orbit
ML-CAPE	Mean Layer CAPE
ML-ECAPE	Mean Layer Entrainment CAPE

OAR	Oceanic and Atmospheric Research
PBL	Planetary Boundary Layer
PSL	Physical Sciences Laboratory
RO	Radio Occultation
SDAD	Standard Deviation of the Absolute Difference
SDD	Standard Deviation of the Difference
SNR	Signal to Noise Ratio
TEMP	Temperature
UCAR	University Corporation for Atmospheric Research
w	Vertical Velocity

ACKNOWLEDGMENTS

Ephesians 3:20–21

THIS PAGE INTENTIONALLY LEFT BLANK

I. INTRODUCTION

A. BACKGROUND

The primary composition of the Earth's atmosphere consists of three permanent gases: nitrogen, oxygen, and argon. However, the atmosphere's composition constantly changes in space and time with other variable and trace gases. The concentration of water vapor varies from zero to four percent in the atmosphere. This concentration is relatively small, but its impact on the atmosphere is colossal.

Water is the only substance that exists naturally in the atmosphere in three phases: gas, liquid, and solid. Phase change results in a transfer of energy, which creates energy cycles in the atmosphere. The hydraulic cycle is the circulation of water through these phases from its existence on the surface to the atmosphere and back to the land (Ackerman and Knox 2015). Clouds that form from the condensation of water vapor are a significant source of uncertainty in global weather forecasts and climate models. Quantifying how accurately these numerical models capture the vertical distribution of water vapor is vital in identifying sources of uncertainty in predicting clouds. Knowing the uncertainties can drive further research into understanding the mechanism and processes contributing to the hydrologic cycle. This thesis focuses on measuring the uncertainty of modeling the variable gas water vapor in the atmosphere and demonstrating the potential impacts caused by the uncertainty through model experiments.

We use Global Navigation Satellite Systems (GNSS) data to depict the atmosphere's state and then compare it with a numerical reanalysis model to quantify the uncertainty of moisture. GNSS are constantly orbiting the Earth in a Medium Earth Orbit (MEO) at an altitude of approximately 20,200 km. GNSS satellites in MEO continuously direct signals towards Earth for terrestrial users, but some signals are bent or refracted back into space (National Coordination Office for Space-Based Positioning, Navigation, and Timing, 2020). Atmospheric research can leverage these signals as they are occulted or cut off from reaching the ground. The Earth's atmosphere causes these signals to refract back into space. Occultations occur when there is a change in temperature, pressure, or electron

density in the atmosphere. GNSS satellites and Low Earth Orbiting (LEO) satellites must have the correct positioning so that transmitting signals pass through the Earth's atmosphere and are refracted towards LEO satellites equipped with the proper equipment to receive these radio waves, Radio Occultations (RO). From here the signals are transmitted to ground stations for processing and dissemination. Through the bending of GNSS signals by the atmosphere RO data can capture accurate and precise profiles or atmospheric soundings of water vapor, temperature, and pressure. The Constellation Observing System for Meteorology, Ionosphere, and Climate (COSMIC) is a network of satellites designed to capture these bent signals and convert them to accurate atmospheric profile soundings (Ho et al. 2020a).

The COSMIC program is a University Corporation for Atmospheric Research (UCAR) initiative, which dates to the initial RO missions of the 1990s. Through their success in the collection and scientific application of GNSS data has enabled follow-on missions. COSMIC-2/FORMOSAT-7 (hereafter COSMIC-2) is the active mission of U.S. agencies and Taiwan's National Space Organization (UCAR). The composition of COSMIC-2 is six LEO satellites capable of collecting at least 5,000 RO soundings per day from various GNSS transmissions (Ho et al. 2020a). UCAR's COSMIC Data Analysis and Archive Center (CDAAC) processes raw data and distributes it near-real-time (CDAAC 4.7 2020). This thesis leverages the archive data provided by CDAAC to investigate the uncertainty of water vapor in the atmosphere.

Research using RO has proven to be successful in various atmospheric processes. However, before the recent launch of COSMIC-2 in 2019, there have been significant issues over oceans in the lower tropical troposphere because of the sharp planetary boundary layer (PBL). COSMIC-2 satellites have a new receiver, the TriG (GPS, GALILEO, and GLONASS) GNSS RO Receiver system. This receiver can increase the signal-to-noise ratio (SNR) by a factor of two (Ho et al. 2020a). With a higher SNR, RO can penetrate the PBL and produce higher quality and quantity atmospheric soundings. Initial findings of COSMIC-2 RO data have resulted with a ~5% increase from previous COSMIC missions with 85% of data penetrating lower than 1km (Ho et al. 2020a). Additionally, RO increases the productivity from one sounding to seven per day. They are

available from 35°N to 35°S in a 5°X 5° latitude box (Ho et al. 2020a). This research uses the high-quality RO sounding from COSMIC-2 to quantify uncertainties of water vapor in the atmosphere and then demonstrate the potential impact of these uncertainties. Hereafter, RO's from COSMIC-2 will be referred to as RO.

According to George Long's translation of Discourses book II, Chapter XVII, the Greek philosopher Epictetus writes: "For it is impossible for anyone to begin to learn that which he thinks he already knows." Numerical models attempt to provide the most accurate representation of the atmosphere in order to provide a deterministic or probabilistic forecast. Reanalysis models strive to offer a comprehensive atmosphere record by blending model forecast and observations (Kanamitsu et al. 2002). However, the uncertainty of the atmosphere is inevitable. It is essential to quantify numerical models' uncertainties to expose where research and development must progress to unfold the processes and mechanisms governing the atmosphere with greater accuracy and precision.

This research aims to quantify the moisture uncertainty in the National Center for Environmental Prediction – Department of Energy Atmospheric Model Intercomparison Project reanalysis model 2 (NCEP-DOE AMIP-II R2), hereafter NCEP. NCEP is an updated and human error-fixed version of NCEP Reanalysis -1 (R-1). The updates to NCEP were minor, and consequently, it is not considered a replacement nor a next-generation reanalysis model of R-1 (Kanamitsu et al. 2002). Currently, a new reanalysis model, NCEP Climate Forecast System Reanalysis (CFSR), is "next generation," but the data corresponding to this study is not publicly released yet. However, this does not discredit the desire to quantify and demonstrate the impact of the moisture uncertainty of NCEP. New and future analyses have the benefit of leveraging lessons learned from the previous reanalysis. Improvement in data assimilation, numerical modeling, and other processes in reanalysis models will be continuous (Thorne and Vose 2010). Moisture uncertainties with the European Center for Medium-Range Weather Forecast (ECMWF) Reanalysis version 5 (ERA5) model will also be explored. ERA5 is a modern reanalysis model and presumably the model uncertainties found in NCEP should be less when examining a newer dataset.

The process of generating a reanalysis output begins with the collection of observations followed by quality control of observations. The next step consists of

assimilation, where spatially and temporally dispersed observations are aligned into a uniform grid. Then the numerical model will use model-specific dynamics and physics to produce an output. This research assesses the model output of NCEP by making a direct comparison to RO observations available in the area of interest (AOI). Due to the abundance of open ocean, the INDOPACOM AOI lacks observations from terrestrial means. Accurate observations are necessary to set the initial conditions of a numerical model and the sparsity of observations is one of the most significant challenges for the AOI. The injection of remote sensing observations, such as RO, can decrease this challenge's impact. Figure 1 depicts the spread of COSMIC-2 observations for one day in the AOI. Figure 2 displays how the availability of RO can increase the observations injected on a monthly scale for a localized area centered with a 5° latitude and longitude of the island of Guam. In addition to the INDOPACOM NCEP vs. RO comparisons, an analysis of the NCEP model output will be assessing in the localized subset area of Guam. The purpose of this subset is to capture localized differences in profiles in an area that is commonly operated by the U.S. Navy.

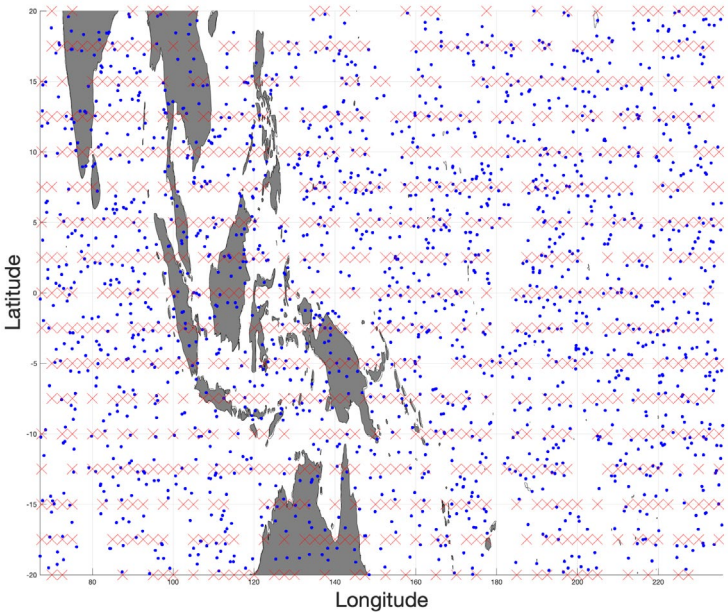

Mean RO observation locations are plotted in blue, and corresponding NCEP-R2 grid points are plotted with a red 'X.' Observations are from May 1, 2020. Figure was created using MATLAB R2020b.

Figure 1. INDOPACOM RO Observations

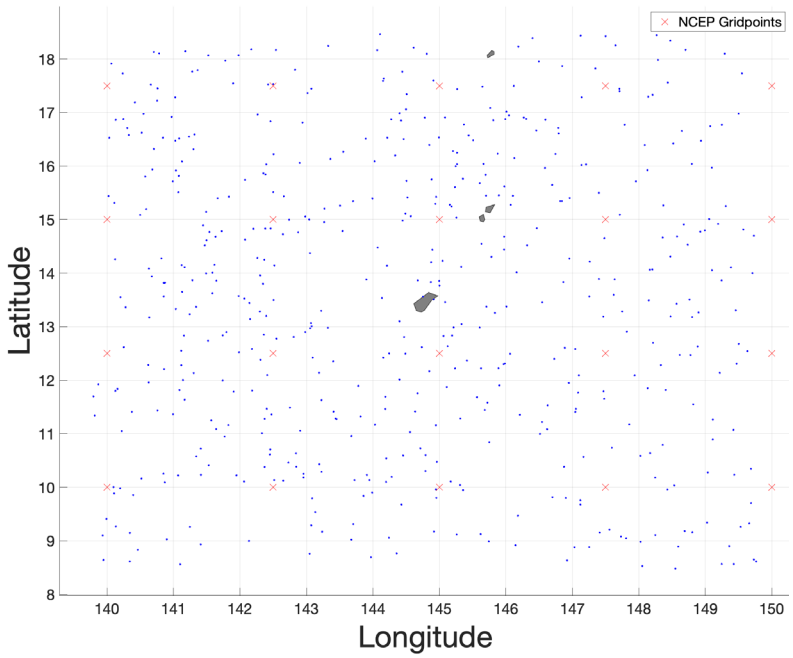

RO observation locations plotted in blue and corresponding NCEP-R2 grid points are plotted with a red 'X.' Observations are for May 2020. Figure was created using MATLAB R2020b.

Figure 2. Guam RO Locations

The Glossary of Meteorology, from the American Meteorological Society (AMS), defines moist convection as:

> Atmospheric convection in which the phase changes of water play an appreciable role. All cumuliform clouds are manifestations of moist convection. The enthalpy exchange between condensing water vapor or freezing liquid water and air is a major contributor to the positive buoyancy of updrafts, while the reverse exchange between air and evaporating water or melting ice contributes strongly to the negative buoyancy of downdrafts. (American Meteorological Society 2012a)

Through deep moist convection, the concentration of water vapor plays a significant role in the vertical distribution of heat through the generation of cumuliform clouds. Therefore, moist convection is a leading method of vertical heat transport, especially in the tropics. Through this vertical heat redistribution, water vapor is a regulator of planetary temperatures through absorption and emission of radiation (American Meteorological Society 2012b). Consequently, knowing the water vapor concentration in

the atmosphere is significant as it can impact large-scale climate teleconnection patterns (Arakawa 2004).

The mixing of a deep convective cloud with their surroundings through entrainment is a key regulating factor on the behavior of deep convective updrafts. When entrainment is large, updraft buoyancy is strongly diluted, and convective clouds remain relatively shallow and dissipate quickly after forming. In contrast, when entrainment is small, updraft buoyancy is only minimally diluted allowing for comparatively strong and persistent updrafts. Entrainment-driven dilution of convection is also strongly dependent on the relative humidity (RH) of the ambient environment, with a drier environment resulting in more updraft buoyancy dilution than a moister environment (Peters et al. 2020; Romps and Kuang 2010; Morrison 2017; Peters et al. 2019). The effects of entrainment on convection are strongly reliant on RH. Variations of RH can determine if deep convection occurs or not. Therefore, it is vital to have an accurate water vapor concentration for improved accuracy in numerical climate and forecast models.

Entrainment is one of the primary sources of uncertainty in cumulus parameterizations, and consequently in global climate prediction (Arakawa 2004). Most reananalyses must also parameterize convection, and reanalysis is therefore susceptible to the same entrainment related errors that climate models experience. Errors related to entrainment have the potential to lead to positive error feedback loops, whereby unrealistically large entrainment results in shallower and less expansive convection, which in turn does not realistically moisten the surrounding environment and makes subsequent convection less likely to occur (Peters et al. 2020a, b).

The calculation of convective available potential energy (CAPE) (M. W. Moncrieff and M. J. Miller 1975) has become a commonly used parameter for forecasting instability in the environment. However, CAPE calculations do not account for entrainment as it only includes a parcels surface temperature and moisture characteristics. Mean Layer CAPE (ML-CAPE) is calculated using the parcels temperature and moisture values from the lowest 100 hPa above ground level (NWS Internet Services Team 2009). ML-CAPE generates calculations more representative of storm's actual effective inflow layers (Nowotarski et al. 2020), but still does not account for entrainment above the effective

inflow layer. This study will calculate mean layer entrainment CAPE (ML-ECAPE) in an effort to better represent the importance of entrainment in vertical velocity of atmospheric profiles (Peters et al. 2020a,b) .

Uncertainty in numerical models is inevitable. The purpose of this thesis is to quantify the uncertainty of moisture and demonstrate the impact of the uncertainty. This is accomplished by the following objectives:

- Use RO to evaluate and quantify the difference of atmospheric profiles between model and observation.
- Determine and calculate bias and magnitude of model and RO differences.
- Compare RO RH and temperature profiles with a modern reanalysis model in order to compare and contrast the uncertainties associated with NCEP and RO.
- Draw comparisons with in-situ observations profiles to demonstrate the differences between modeled NCEP profiles and observed remote sensing profiles of RO.
- Demonstrate the potential impact of the moisture uncertainties in reanalysis on storm behavior, soundings from our analysis are used to run high resolution Cloud Model-1 (CM1) simulations with variable moisture content.

B. MOTIVATION

From an operational and forecasting perspective, moist convection can have a significant impact. At sea, navigators and aviators ensure operations remain outside areas of convection, comically known as “angry clouds.” Aviators tend to avoid areas of deep moist convection because they have strong updrafts creating turbulence, strong icing conditions, and the potential presence of electrification. Navigators at sea can appreciate a “free” freshwater washdown in mild precipitation events but make a stern effort to avoid areas of deep convection. These areas create environments where Navy ships cannot

conduct operations and instead shift focus to survivability with minimal degradation on ship and crew.

In areas of deep moist convection, ships must be "secure for sea," and weather decks are secure to non-essential personnel. Naval theorist Alfred Mahan believed wars are won at sea and not on land. Victory is achieved by command of the sea through decisive battle (Mahan 1949). However, command of the sea is not obtained if the environment limits a Commander's freedom to maneuver. Understanding the deep convection processes can improve forecast accuracy and increase the Commander's ability to maneuver appropriately. The injection of an accurate representation of the environment into the planning phase results in reaching the Commander's desired end state of control of the sea. To get to the desired end state, climatology reports are constructed for planning military operations. These reports are generated using reanalysis data. Knowing the uncertainties and bias of reanalysis models allows users to understand the limitations of the data provided.

For naval operations to occur effectively and efficiently, it is critical to ensure forecast and climate models accurately depict moist convection. However, global reanalysis and forecasting models do not have the horizontal and temporal resolutions to resolve deep moist convection. Because of this limitation, numerical models must rely on cumulus parameterizations to represent the process of deep convection. Deep convection is a mesoscale phenomenon that can develop quickly, and its development may significantly impact nearby synoptic-scale environments through heat and moisture transport (Peters and Roebber 2014). Deep moist convection is, in turn, strongly dependent on atmospheric water vapor concentration (Zhang 2005; Arakawa 2004). This research aims to quantify the uncertainty and bias of NCEP and ERA5. Model simulations will be conducted to express the impact of the uncertainty and bias found in the reanalysis models.

II. METHODS

The United States Department of Defense (DOD) is a global force compartmentalized into six Geographic Combatant Commands (GCC). The GCC of Indo-Pacific Command (INDOPACOM) encompasses nearly half of the world's surface and is the largest operating area for the U.S. Navy. This research quantifies the uncertainty in the middle tropospheric moisture in the tropical portion of INDOPACOM, as seen in Figure 3. The middle troposphere is defined as 850–500 hPa section of the atmosphere, which typically corresponds to the 1–5 km geopotential height range. Convection is sensitive to moisture concentrations in this section of the atmosphere (Derbyshire et al. 2004). Thus, quantifying moisture uncertainty is critical. The area of interest (AOI) extends from 20°N to 20°Swith longitude boundaries of 67°E and 124°W. Quantifying the uncertainty of moisture in the atmosphere can assist in further identifying and understanding the limitations of gridded atmospheric analyses, which are frequently used to both initialize global forecast models, analyze past weather events, and to generate global and regional climate analyses. In addition, our analysis may help identify biases in cumulus parametrizations, which are commonly used in global climate and global forecast models, such as the Navy Global Environmental Model (NAVGEM). These potential moisture biases are of critical importance to Navy operations because they may lead directly to forecast errors that can negatively affect operations.

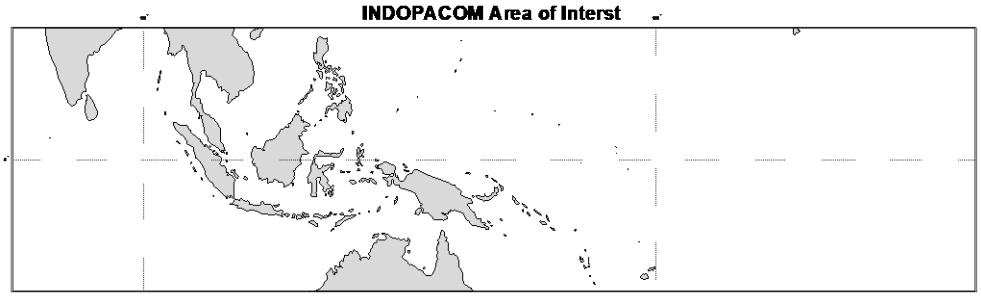

Figure was created using MATLAB R2020b.

Figure 3. INDOPACOM AOI

Figure 4 depicts the monthly rainfall observed at 14 stations on the island of Guam. The NWS forecast office is labeled as GU NWSO, and the climatological recorded is plotted with a red dash line labeled "GU NWSO Norm." May to August was the selected timeframe as it has the highest potential for capturing periods of the most active thunderstorms due the increase accumulation of rainfall. By focusing on this timeframe, we can effectively demonstrate through model simulations how moisture uncertainties may influence forecasts of thunderstorms. For instance, a bias in analyzed moisture might result in the erroneous behavior of parametrized convection in the reanalysis model. This could translate in a tendency for analyses forecasts to have too little convective activity, because these models misrepresent the deleterious effects of entrainment on updraft buoyancy.

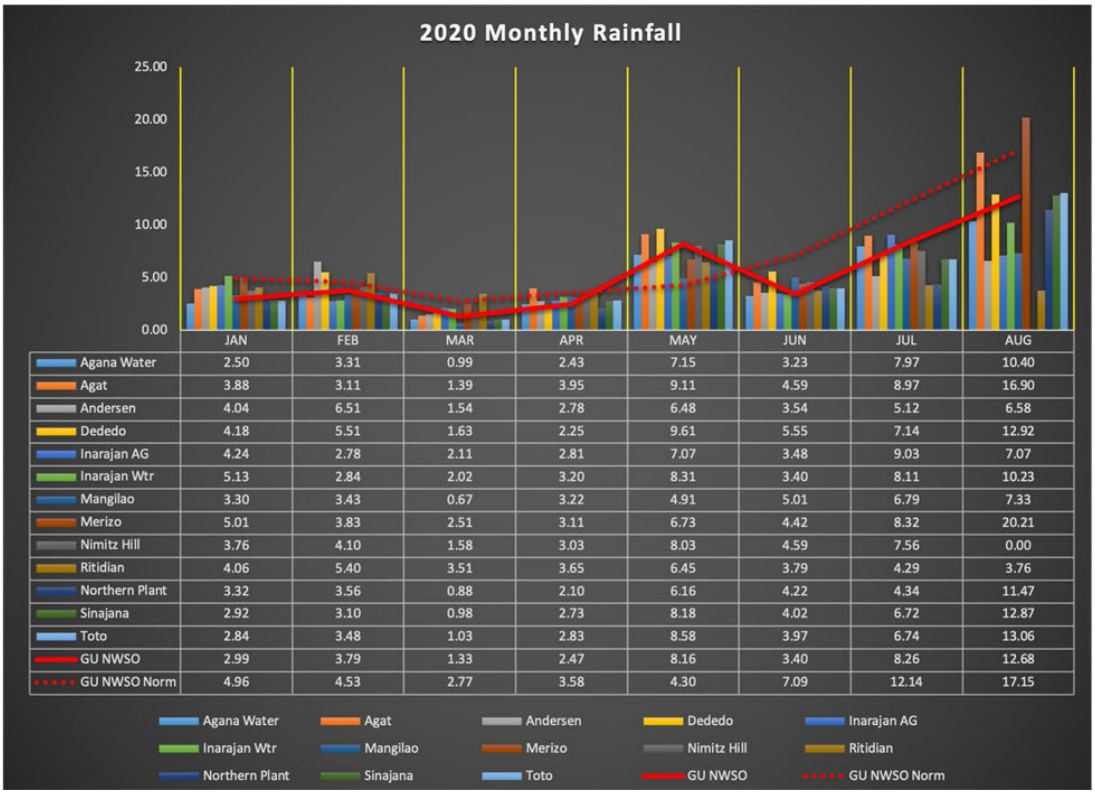

	JAN	FEB	MAR	APR	MAY	JUN	JUL	AUG
Agana Water	2.50	3.31	0.99	2.43	7.15	3.23	7.97	10.40
Agat	3.88	3.11	1.39	3.95	9.11	4.59	8.97	16.90
Andersen	4.04	6.51	1.54	2.78	6.48	3.54	5.12	6.58
Dededo	4.18	5.51	1.63	2.25	9.61	5.55	7.14	12.92
Inarajan AG	4.24	2.78	2.11	2.81	7.07	3.48	9.03	7.07
Inarajan Wtr	5.13	2.84	2.02	3.20	8.31	3.40	8.11	10.23
Mangilao	3.30	3.43	0.67	3.22	4.91	5.01	6.79	7.33
Merizo	5.01	3.83	2.51	3.11	6.73	4.42	8.32	20.21
Nimitz Hill	3.76	4.10	1.58	3.03	8.03	4.59	7.56	0.00
Ritidian	4.06	5.40	3.51	3.65	6.45	3.79	4.29	3.76
Northern Plant	3.32	3.56	0.88	2.10	6.16	4.22	4.34	11.47
Sinajana	2.92	3.10	0.98	2.73	8.18	4.02	6.72	12.87
Toto	2.84	3.48	1.03	2.83	8.58	3.97	6.74	13.06
GU NWSO	2.99	3.79	1.33	2.47	8.16	3.40	8.26	12.68
GU NWSO Norm	4.96	4.53	2.77	3.58	4.30	7.09	12.14	17.15

Recorded rainfall accumulation in inches for observation stations in Guam (GU). Sold red line is the Guam National Weather Service Office (N`WSO) reported total. Dash red line is the climatological average for GU NWSO. Source: US Department of Commerce (2020).

Figure 4. Guam NWS Forecasting Office Recorded Rainfall (Inches)

This study uses the NCEP data provided by National Oceanographic Atmospheric Administration (NOAA) Oceanic and Atmospheric Research (OAR) Earth System Research Laboratories (ESRL) Physical Sciences Laboratory (PSL) from Boulder, Colorado, USA through their website: https://psl.noaa.gov/data/gridded/data.ncep.reanalysis2.pressure.html. We constructed atmospheric profiles from NCEP for our AOI using the air temperature and RH files with a temporal coverage of four times daily with a grid spacing of 2.5° latitude by 2.5° longitude global grid.

RO data are available via CDAAC from as early as March 2019 to the present. Since the launch of COSMIC-2 is relatively recent at the beginning of this study, May 2020 to August 2020 is the study's timeframe. To further analyze the uncertainty of moisture in NCEP, a subsection of the AOI was chosen centered on and with 5° latitude and longitude of the island of Guam. At this location, radiosonde launches occur daily at 00 UTC and 12 UTC, which is the reason for our focus on this area. In our analysis, we will compare the RO and NCEP profiles to radiosonde observations; this allows us to compare the accuracy of the RO and NCEP. This step is important because this study uses RO to gauge the accuracy of NCEP in regions where radiosonde observations are unavailable, and this assessment hinges on the RO profiles having accurate temperature and moisture representation of the atmosphere. In the radiosonde comparison with RO, we will only evaluate profiles within 110 km of the radiosonde site, which corresponds to roughly 1 degree of latitude. This distance is selected because it is comparable to the 111 km distance between the center of the closest NCEP grid point and the radiosonde launch site

Radiosonde data from the Guam international airport were retrieved from the University of Wyoming College of Engineering department of Atmospheric Science archive (Oolman 2020). Observations from weather balloon launches were recorded daily at 00 UTC and 12 UTC for the desired research period. Data on July 2, 2020 were not available.

In addition to quantifying the difference moisture uncertainties in NCEP, we will quantify the uncertainty in derived quantities that depend on moisture such as CAPE and entrainment CAPE (ECAPE). To compute CAPE, we adiabatically lifted parcels from each height between the surface and 1 km, using the method described in Peters et al. (2021).

We then averaged the buoyancy of each of these lifted parcels, and computed CAPE from this resulting averaged buoyancy. This is akin to the traditional "mean-layer" CAPE calculation, which lifts a parcel with the average properties of the lowest 100 hPa of the atmosphere and computes CAPE for this lifted parcel. Thus, we refer to our CAPE calculation as "ML-CAPE." The ECAPE calculation also follows the method of Peters et al. (2021), with an assumed fractional entrainment rate of $5x10^{-4}$ ms^{-1}, which corresponds to an assumed updraft width of approximately 3 km. ECAPE calculations will be referred to as ML-ECAPE.

RO profiles from May to August were obtained from CDAAC level 2 atmospheric profiles were from the wetPrf2 dataset using the 1D-var retrieval method. The wetPrf2 dataset retrieval method includes moisture in the profile, and it is interpolated to 100-meter height levels (CDAAC 4.7 2020). The INDOPACOM AOI is in the tropics and in this environment, RO is known to have a negative bias in the lower moist troposphere, near the PBL. The bias is caused by the sharp vertical moisture gradients that result in superrefraction (Ho et al. 2007). To account for the known negative RO bias in the lower troposphere, wetPrf2 retrievals uses a gridded analysis or short term forecast to reduce the observation error (CDACC 4.7 2020; Ho et al. 2020b). Therefore, RO wetPrf2 profiles can be greatly influenced to fit the priori background atmosphere, especially below 2km (Ho et al. 2020b). However, the profiles used in this research are from 850–500 hPa, which is primarily above 2km and thereby making the background influence negligible. In the tropics the 850 hPa contour is typically near 1 km. Additional information on the 1D-var retrieval method can be found at: https://cdaac-www.cosmic.ucar.edu/cdaac/doc/documents/1dvar.pdf.

For this study, RO data were first filtered by selecting profiles within the INDOPACOM AOI. Then the profiles were trimmed from 1000 hPa to 50 hPa to eliminate the data above the tropical troposphere where water vapor concentrations are negligible. The RO data was divided into time segments that were within three hours of NCEP output. Due to the variable availability of data to assimilate into a forecast model, data assimilation processes are constantly changing for forecast models. However, reanalysis models such as NCEP have a constant physics, dynamics, and data assimilation system to eliminate

climate bias (Saha et al. 2010). Because of this constant data assimilation in NCEP, RO atmospheric profiles are not included in the reanalysis model. This exclusion is important as it allows RO to be an independent variable. To assess further assess the validity of RO, a comparison was explored using the comparatively modern and high-resolution European Centre for Medium-Range (ECMWF) Weather Forecasts Reanalysis 5 (ERA5) (Hersbach et al., 2018).

In this research we compare moisture profiles from a) NCEP vs. RO, b) ERA5 vs. RO, c) NCEP vs. radiosonde, and d) radiosonde vs. RO. The comparison of NCEP and RO seeks to demonstrate the uncertainty of moisture by quantifying the differences in these profiles. Radiosonde observations have comparatively low error ranges (Ho et al. 2020b). Therefore, the NCEP and RO comparisons with radiosonde allow us to gauge the relative accuracies of the reanalysis and RO. Additionally, radiosonde observations are assimilated into the reanalysis models therefore, the NCEP vs. radiosonde comparison gives a sense of uncertainty between model an assimilated observation. The ERA5 vs. RO comparisons will also demonstrate the differences between model and assimilated data. In addition to quantifying the moisture uncertainty, a comparison of temperature profiles will also be calculated. These temperature comparisons demonstrate how well NCEP, RO, and radiosonde temperature recordings are aligned. Model simulation comparisons will be conducted to highlight the impact of the moisture uncertainties between NCEP and RO.

A. METHODS FOR COMPARISONS

The comparisons mentioned above are created by binning RO data into four time outputs of 00Z, 06Z, 12Z, and 18Z. RO profiles within three hours of the bin output time frames were grouped together. RO profiles are then compared to the closest NCEP grid point. RO have a horizontal resolution which varies from 100–300km (Ho et al. 2020a; Biondi et al. 2011; Kursinski et al. 1997), therefore the mean latitude and longitude was used as the RO position. This caveat is negligible given that the horizontal resolution of the RO is comparable to the NCEP horizontal resolution of ~277km. ERA5 has a much higher spatial resolution of nominally 30km (Hersbach et al. 2020, Hershcah et al. 2018). To account for this all ERA5 grid points with centers located inside a box bounded by the

maxima and minima latitudes and longitudes sampled by RO between 850 and 500 hPa were averaged to obtain the ERA5 profile that was then compared to RO. RO profiles within 3 hours and 111 km from the radiosonde were used to make radiosonde vs. RO comparisons. 111km was selected as the maximum distance because it is the distance between the radiosonde launch location and the closest NCEP grid point.

Profiles of RO, NCEP, ERA5 and radiosondes were further trimmed from 800–500 hPa. This section of the atmosphere was chosen because variations found here can significantly impact entrainment-driven dilution of updraft buoyancy in thunderstorms (e.g., Derbyshire et al. 2004; Wang and Sobel 2012). To quantify the differences between NCEP and the observed environment the following calculations are conducted via Equations 1–6: BIAS, Standard Deviation of the Difference (SDD), Mean Absolute Difference (MAD), and Standard Deviations of the Absolute Difference (SDAD) via Equations 1 through 4.

$$BIAS = \frac{1}{N}\sum_{n=1}^{N}(Model_n - Observation_n) \quad (1)$$

$$SDD = \sqrt{(\frac{1}{N}\sum_{n=1}^{N}[BIAS - (Model_n - Observation_n)]^2} \quad (2)$$

$$MAD = \frac{1}{N}\sum_{n=1}^{N}|Model_n - Observation_n| \quad (3)$$

$$SDAD = \sqrt{(\frac{1}{N}\sum_{n=1}^{N}[MAE - |Model_n - Observation_n|]^2} \quad (4)$$

In these equations, "*N*" is the total number of profiles and "*n*" is the index of individual profiles. In addition, a Student's t-test was conducted on the BIAS and MAD. Confidence intervals are the 5th-to-95th percent confidence bounds based on a Student's t-test. For single valued metrics such as BIAS, both confidence bounds were required to be same signed for a bias to be statistically significant (i.e., $p < 0.05$). Differences between two values in a comparison were statistically significant if the confidence bounds of respective variables did not overlap. BIAS and MAE confidence intervals (CI) are also calculated. Composite is defined as the aggregating of data from the entire time span of the research, May to August 2020. The distribution of the results resembles aspects of a normal

distribution, and this is a caveat to using the metric and analysis drawn from the Student's t-test metrics.

From the collected profiles, the following comparisons are made: INDOPACOM NCEP vs. RO, INDOPACOM ERA5 vs. RO, Guam NCEP vs. RO, Guam ERA5 vs. RO, Guam NCEP vs. radiosonde, and Guam Radiosonde vs. RO. When calculating the Radiosonde vs. RO comparison, the radiosonde value is replacing the "Model" position in Equations 1–4. In addition, to capturing moisture differences in profiles, monthly and composite temperature profiles are also compared. The same equations and process used to capture the moisture differences is used to quantify the uncertainty in temperature profiles.

Section III.D provides normalized (NORM) BIAS and MAD values via Equations 5 and 6 for INDOPACOM and Guam NCEP vs. RO, NCEP vs. radiosonde, and radiosonde vs. RO comparisons. Normalization is conducted by dividing by the observation sample size median. The observed sample size median was selected to for normalization because it is a robust metric that is not sensitive to outliers (Wilks 2006). To capture the thermodynamic impacts potentially caused by the temperature and RH uncertainties, composite ML-CAPE and ML-ECAPE comparisons are calculated to using Equations 1–6. When calculating the ML-CAPE and ML-ECAPE NORM calculations, only profiles that exceeded a ML-CAPE value of 100 J kg^{-1} or greater are considered.

$$NORM\ BIAS = \left(\frac{1}{N}\sum_{n=1}^{N} NCEP_n - Observation_n\right)\ Median\ of\ Obs_N\ ^*100 \qquad (5)$$

$$NORM\ MAE = \left(\frac{1}{N}\sum_{n=1}^{N} |NCEP_n - Observation_n|\right) Median\ of\ Obs_N * 100 \qquad (6)$$

B. CONFIGURATION FOR CLOUD MODEL EXPERIMENT

This research uses Cloud Model 1 (CM1) to demonstrate the impact of atmospheric profile differences of NCEP and RO. CM1 is a non-hydrostatic cloud model developed by George Bryan at the Pennsylvania State University (e.g., Bryan and Fritsch 2002), and currently maintained at the National Center for Atmospheric Research. We use this model

to run idealized simulations with variations in moisture that are comparable to the uncertainty in the NCEP reanalysis, and to demonstrate the impact of these moisture variations in the intensity of the simulated thunderstorms.

Our model domain was cubic, with a grid length of 25 km in the x, y, and z directions. The horizontal and vertical grid spacing was 100 m. The initial and lateral boundary conditions were uniformly set to a single thermodynamic profile from one of the radiosonde launches at Guam, as will be discussed later. Convection was initiated by first applying random temperature perturbations to the model domain with maximum amplitudes of 0.25 K, and then applying spatially uniform surface potential temperature and water vapor mixing ratio fluxes of 0.03 K m^{-2} and 1x10-5 m^{-2} respectively for 1 hour, to spin up a turbulent PBL. After one hour, a Gaussian shaped region of enhanced fluxes was applied to the domain center with a maximum amplitude of 20 times that of the initial horizontally uniform flux, and a radius of influence of 5 km. This locally enhanced flux generated sufficient local buoyancy with the PBL to initiate deep convection.

Table 1 provides the model configuration for CM1. The input sounding for CM1 was constructed from a radiosonde launch in Guam on 13 August 2020. This sounding was chosen because a considerable amount of convection was present in the surrounding environment at the time of the radiosonde launch. After the initial CM1 simulation, the sounding's RH was altered at the 800–500 hPa section of atmospheric column using a process that will be discussed later.

Table 1. CM1 Model Configuration

Attribute	Value/Setting	Notes
Fully Compressible	Yes	
Horizontal Grid Spacing	100 m	
Vertical Grid Spacing	100 m	
Vertical Coordinate	Height (m)	
Number of x, y, and z Points	250 x 250 x 250	
Vertical Points	180	
Top/Bottom LBCs	Free-slip	
North/South LBCs	Open-radiative	Durran and Klemp (1983)
East/West LBCs	Open-radiative	Durran and Klemp (1983)
Microphysics	Morrison	Morrison et al. (2009)
Diffusion	6th order	
Subgrid Turbulence	TKE	
Rayleigh Dampening	Yes	
Dissipative Heating	Yes	
2nd and 6th Order Coef.	75-.04	
Longwave Radiation	None	
Shortwave Radiation	None	
Surface Layer	None	
Boundary Layer Physics	None	
Cumulus Parameterization	None	

THIS PAGE INTENTIONALLY LEFT BLANK

III. RESULTS

A. REANALYSIS MODEL VS. RO COMPARISON

The primary objective of this study is to quantify moisture uncertainty in NCEP. This is accomplished by making comparisons with RO. ERA5 vs. RO comparisons are constructed to demonstrate any potential differences in uncertainty in a new model that assimilates RO.

1. Model vs. RO Comparison in INDOPACOM

The monthly and composite calculations for the INDOPACOM NCEP vs. RO RH comparison of profiles from 850–500 hPa are listed in Table 2. The INDOPACOM results with a composite negative RH BIAS of -3.64% with monthly ranges from -1.79% to -5.29%. Negative RH BIAS are associated with models having a "dry" BIAS. A dry BIAS equates to the model showing less moisture than the sampled atmosphere. The BIAS CI all have a range less than half a percent, which is small compared to the Guam ranges shown below because of the large sample size of the INDOPACOM AOI. From Table 2, there is a consistent RH BIAS increasing in magnitude from May to July, but August results with the smallest RH BIAS of -1.79%. However, August has the greatest RH MAD of 20.35% and SDAD of 14.98%. The RH MAD in NCEP vs. RO profiles are considerably larger than the BIAS with a composite MAD value of 17.93% and monthly MAD ranging from 16.24% to 20.35%. The RH MAD composite SDAD is 13.62%.

Table 2. INDOPACOM - NCEP vs. RO - RH (%)

	May	June	July	August	Composite
Occurrences	42432	34306	37080	41249	155067
BIAS	-3.05	-4.80	-5.29	-1.79	-3.64
BIAS CI	-3.24 to -2.85	-5.02 to -4.6	-5.51 to -5.07	-2.03 to -1.55	-3.75 to -3.53
SDD	20.60	20.95	21.41	25.21	22.22
MAD	16.24	17.23	17.83	20.35	17.93

	May	June	July	August	Composite
MAD CI	16.10 to 16.35	17.09 to 17.36	17.69 to 17.96	20.20 to 20.49	17.86 to 17.99
SDAD	13.03	12.85	12.98	14.98	13.62

Table notes: A Student's t-test was conducted for the monthly and composite BIAS and MAD data sets. All student t-test resulted with data being statistically significant and P-value of zero.

The BIAS distribution is displayed in box plots and seen in Figure 5. Here we see the monthly variability is consistent with a RH SDD range from 20.60% to 25.21% and a composite of 22.22%. The monthly distribution of the RH SDAD is consistent with a range of 12.98% to 14.98%. The BIAS and MAD values are statistically significant. Therefore, it is evident a dry RH BIAS exists, meaning NCEP RH values are consistently less than the RO observations. The RH MAD from Table 2 reveals that the monthly magnitude of the profile difference is greater than 16% with monthly CI ranging from 16.10% to 20.49%.

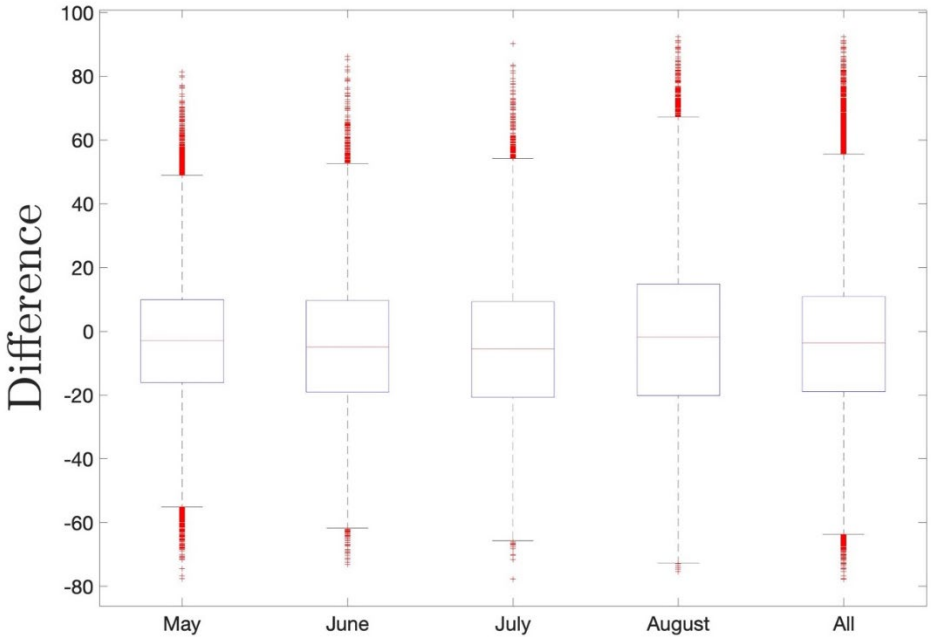

Figure 5. INDOPACOM - NCEP vs. RO - RH (%) BIAS Spread Distribution

The ERA5 INDOPACOM RH analysis results are in Table 3. The RH BIAS are positive, meaning the reanalysis depicts a higher RH than the observed RO. Since there is a higher RH in the analysis than the observation, this is classified as a "wet" BIAS. The magnitude of the wet BIAS in ERA5 exceeds the magnitude RH dry BIAS in NCEP. Interestingly, the modern ERA5 model output has a greater RH BIAS than NCEP, but the magnitude of the moisture uncertainty is greater in NCEP since the MAD are larger. The NCEP and ERA5 vs. RO comparison results of SDD and SDAD calculations include standard deviation and 12 of the 20 values of SDD and SDAD exceed 15%. Therefore, this is a large spread found in the calculated differences. These results encourage exploration to expose locations that exceed 15% RH difference when the reanalysis outputs are compared with RO, section III.A.2.

Table 3. INDOPACOM - ERA5 vs. RO - RH (%)

	May	June	July	August	Composite
Occurrences	43298	34174	35835	41065	154372
BIAS	5.53	7.45	9.09	6.46	7.02
BIAS CI	5.37 to 5.68	7.26 to 7.64	8.89 to 9.28	6.28 to 6.65	6.94 to 7.12
SDD	16.35	17.96	18.82	19.00	18.06
MAD	11.21	12.37	13.17	12.76	12.34
MAD CI	11.09 to 11.34	12.24 to 12.53	13.00 to 13.34	16.61 to 12.91	12.26 to 12.41
SDAD	13.11	14.99	16.23	15.49	14.95

Table notes: A Student's t-test was conducted for the monthly and composite BIAS and MAD data sets. All student t-test resulted with data being statistically significant and P-value of zero.

The magnitude of SDD in ERA5 is less than NCEP. Therefore, the distribution of the BIAS is less in ERA5. This is evident in Figure 6 where the composite reanalysis RH BIAS are shown via a histogram of the calculated differences. The magnitude of the MAD for ERA5 vs. RO RH comparison is less than NCEP vs. RO comparison. The composite MAD for ERA RH comparison with RO is 12.34% compared to NCEP vs. RO composite RH MAD of 17.93%.

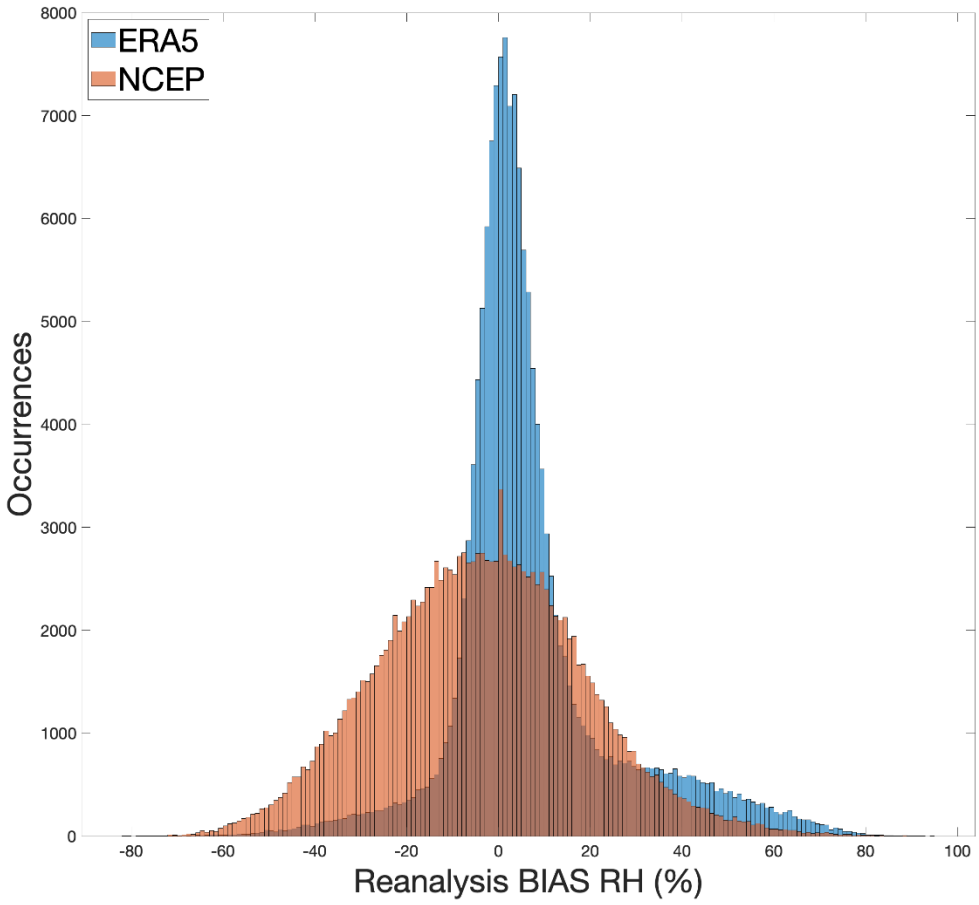

A histogram of the calculated RH differences (Reanalysis minus RO). ERA5 is plotted in blue and NCEP is in red. Abscissa is the percent of BIAS difference and on the ordinate is the number of occurrences. 155067 NCEP vs. RO differences were calculated and 154,372 ERA5 vs. RO.

Figure 6. INDOPACOM Composite Reanalysis RH BIAS

The NCEP vs. RO comparison of temperature profiles from 850–500 hPa is listed in Table 4. This comparison reveals a slight negative temperature BIAS. Similar to the RH comparisons, RO profiles record a higher temperature than NCEP profiles. However, the range of the monthly BIAS is small, and via the SDD, we see the monthly spread of differences has a range from 0.91°C to 1.21°C. The BIAS and MAD results in Table 4 are statistically significant.

Table 4. INDOPACOM - NCEP vs. RO - Temperature °C

	May	June	July	August	Composite
Occurrences	42432	34306	37080	41249	155067
BIAS	-.10	-0.21	-0.14	-0.34	-.20
BIAS CI	-0.11 to -0.09	-0.22 to -0.20	-0.15 to -0.13	-0.35 to -0.33	-.20 to -.19
SDD	1.01	0.91	0.95	1.21	1.04
MAD	0.65	0.64	0.64	0.88	0.71
MAD CI	0.65 to 0.66	0.63 to 0.64	0.63 to 0.65	0.87 to .89	.70 to .71
SDAD	0.78	0.68	0.72	0.90	0.79

Table notes: A Student's t-test was conducted for the monthly and composite BIAS and MAD data sets. All t-test resulted with data being statistically significant and P-value of zero.

The metrics in Table 4 are notable because as temperature increases, a parcel's ability to hold water vapor liquid increases. The Clausius-Claperyon equation finds at temperatures of the lower troposphere, the saturation vapor pressure increases by approximately seven percent for every one-degree increase in temperature (Held and Soden 2006). Figure 7 depicts there is a slight variation of the BIAS temperature comparison. The MAD composite and monthly metrics found Table 4 result in differences of less than one degree.

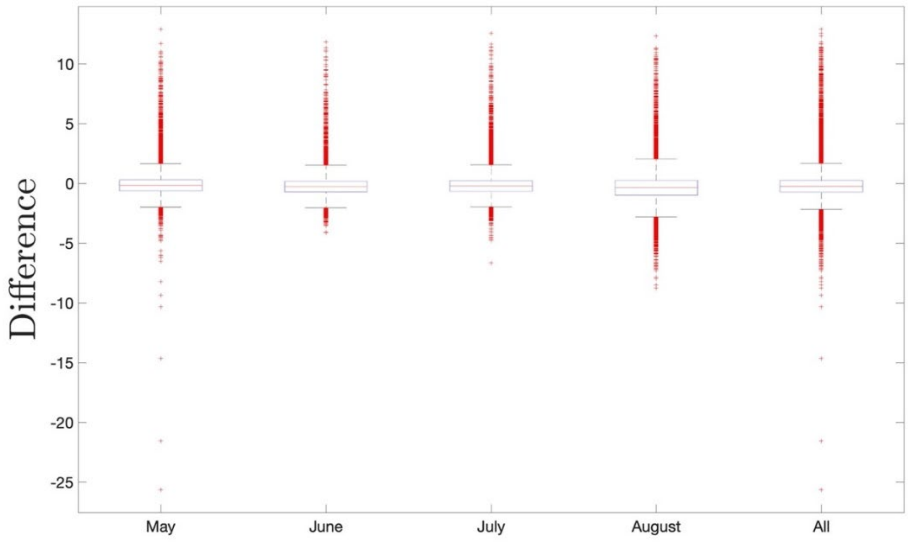

Figure 7. INDOPACOM - NCEP vs. RO - Temperature Spread Distribution

Surprisingly the temperature BIAS and SDD of ERA5 vs. RO are greater in magnitude than the NCEP vs. RO results. The comparison of this study focuses on the 850–500 hPa section of the atmosphere and previous RO studies have concluded RO temperature profiles are most accurate above 8km (e.g., Ho et al. 2020b). Especially below 5 km, relative humidity and temperature retrieved by RO tend to be lower than those observed by radiosondes launched at approximately at the same time and location. However, given the small sample size of co-located RO and radiosonde profiles in this analysis, it is impossible to quantify the mean bias of RO observations compared to reliably accurate sonde observations. Therefore, it is unclear to what extent the differences between ERA5, and RO temperature should be attributed to errors in the RO retrieval and problems with ERA5 physics. The exact reasons for the existence of the large BIAS and MAD temperature values with ERA5 are unclear and are beyond the scope of this study.

Table 5. INDOPACOM - ERA5 vs. RO - Temperature °C

	May	June	July	August	Composite
Occurrences	43298	34174	35835	41065	154372
BIAS	2.44	2.32	2.25	2.24	2.32
BIAS CI	2.43 to 2.45	2.31 to 2.33	2.4 to 2.56	2.22 to 2.5	2.31 to 2.32
SDD	1.19	.96	.99	1.04	1.06
MAD	2.46	2.33	2.26	2.26	2.33
MAD CI	2.45 to 2.48	2.32 to 2.34	2.25 to 2.27	2.25 to 2.27	2.33 to 2.34
SDAD	1.16	.94	.97	.99	1.03

Table notes: A Student's t-test was conducted for the monthly and composite BIAS and MAD data sets. All t-test resulted with data being statistically significant and P-value of zero.

2. Reanalysis model vs. RO comparisons in Guam

The Guam comparisons provides a localized impact that is not seen in the INDOPACOM analysis. The Guam NCEP vs. RO RH comparison results are in Table 6. A Student's t-test revealed the monthly and composite BIAS and MAD results were statistically significant. The monthly and composite RH BIAS values for Guam are larger than the results for INDOPACOM in Table 2. The monthly RH BIAS ranges is from -1.2%

to -25.81% with a composite of -14.02%. The Guam BIAS values are an order of magnitude greater than the BIAS of INDOPACOM. Guam and INDOPACOM NCEP vs. RO comparisons both show a negative BIAS. The negative RH BIAS indicates NCEP values are consistently less than the observed RO observations. To reiterate, all confidence intervals are on the 5th to 95th percent confidence bounds based on the Student's two-tailed t-test. Guam's BIAS results are statistically significant because the monthly and composite BIAS results for the Guam NCEP vs. RO comparisons are outside the corresponding INDOPACOM BIAS CI. A caveat to the statistical significance is the relatively small sample size of Guam and the distribution was not entirely normal.

Guam's monthly RH SDD range from 10.69% to 14.77%, with a composite value of 16.63%. These RH SDD results are less than the INDOPACOM values which range from 20.60% to 25.21%. Therefore, the SDD of Guam shows a reduced amount of spread in the differences for RH in the NCEP vs. RO comparison. However, the GUAM BIAS results are all within one SDD of the INDOPACOM SDD. Finding localized results of moisture uncertainties in INDOPACOM is valuable. These quantifiable uncertainties provide military decision makers a metric to guide their plans and operations conducted in the area.

Table 6. Guam - NCEP vs. RO - RH (%)

	May	June	July	August	Composite
Occurrences	760	593	550	760	2663
BIAS	-1.2	-12.17	-25.81	-19.75	-14.02
BIAS CI	-2.24 to -0.181	-13.40 to -11.10	-26.84 to -25.07	-20.86 to -18.75	-14.73 to -13.45
SDD	14.35	14.45	10.69	14.77	16.63
MAD	11.13	15.38	25.9	21.43	18.07
MAD CI	10.55 to 11.85	14.57 to 16.34	25.18 to 26.91	20.62 to 22.36	17.69 to 18.61
SDAD	9.13	10.98	10.47	12.20	12.12

Table notes: A Student's t-test was conducted for the monthly and composite BIAS and MAD data sets. All t-test resulted with data being statistically significant and P-value of zero.

The May, June, and July RH MAD in Guam are all outside the MAD CI for the corresponding INDOPACOM MAD monthly values. Therefore, the NCEP vs. RO RH MAD for GUAM suggest there is significantly moisture uncertainty than the corresponding INDOPACOM calculations. All of the RH MAD in Guam's are within INDOPACOM's SDAD.

The number of outliers for each NCEP vs. RO comparison is displayed in Figure 5 and Figure 8. The larger spread, greater variation, and negative RH BIAS of the Guam NCEP vs. RO RH comparison results are seen in Figure 8. The Guam distribution spread in Figure 8 displays localized variations which are not present in the to the INDOPACOM equivalent plot, Figure 5. Both figures show a similar spread with similar interquartile ranges, but the medians have a greater monthly variation in the Guam RH comparison. The variation in the magnitude of the negative RH BIAS is also captured in Figure 8, with Guam showing a RH BIAS.

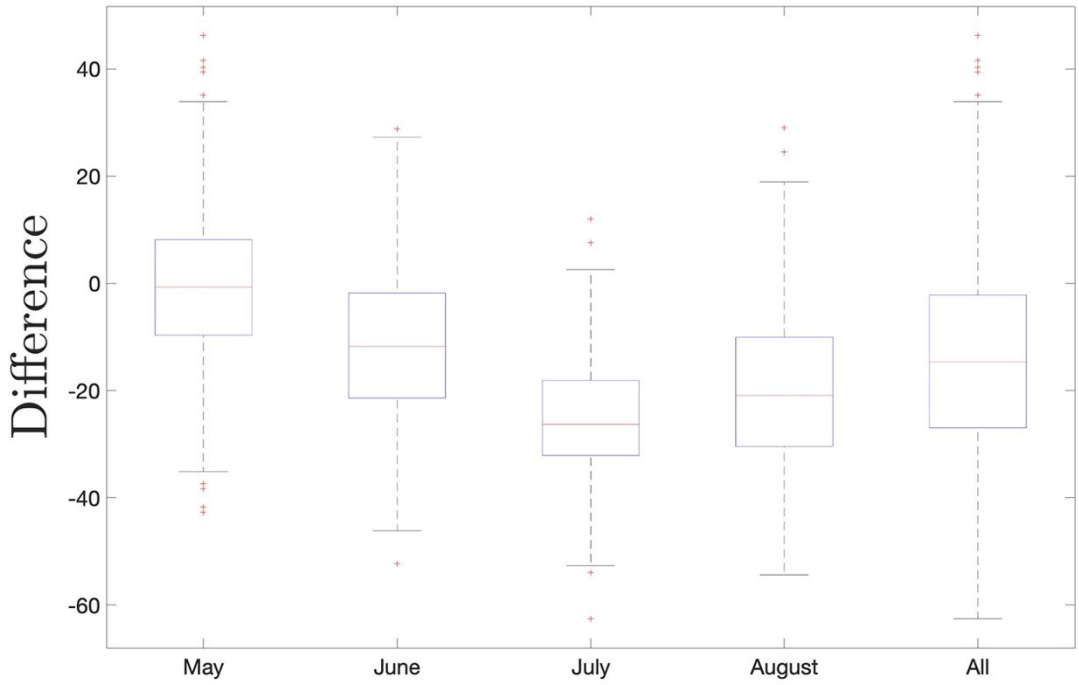

Figure 8. Guam - NCEP vs. RO - RH (%) Distribution Spread

The Guam ERA5 vs. RO RH comparison results are available in Table 7. The RH ERA5 monthly and composite BIAS in Guam are less than the results found in the INDOPACOM ERA5 vs. RO comparison. Each RH BIAS result in Guam is outside the BIAS CI of INDOPACOM. The Gaum RH MAD results are also outside the MAD CI for the INDPACOM ERA analysis as seen when analyzing the associated results in Table 3 and Table 7.

Table 7. Guam - ERA5 vs. RO - RH (%)

	May	June	July	August	Composite
Occurrences	616	471	471	596	2154
BIAS	4.11	3.5	0.87	1.03	2.42
BIAS CI	3.61 to 4.61	3.01 to 4.01	0.43 to 1.03	0.62 to 1.44	2.18 to 2.66
SDD	6.30	5.55	4.83	5.11	5.7
MAD	5.85	5.30	3.8	4.10	4.80
MAD CI	5.48 to 6.22	4.94 to 5.65	3.52 to 4.08	3.84 to 4.36	4.63 to 4.96
SDAD	4.71	3.87	3.10	3.21	3.9

Table notes: A Student's t-test was conducted for the monthly and composite BIAS and MAD data sets. All t-test resulted with data being statistically significant and P-value of zero.

The wet BIAS found in INDOPACOM is present in Guam, but overall, the ERA5 model output is more aligned with the observed RO in this localized area. The Guam MAD ERA5 results show the magnitude of the amount moisture uncertainty is less in Guam than in INDOPACOM. The ERA5 Guam RH comparison with RO BIAS and MAD results are within the ERA5 INDOPACOM SDD and SDAD, respectively. When comparing the NCEP and ERA5 RH SDD we see ERA5 has less spread in the difference results with RO. This is evident in Figure 9, where the NCEP differences seen in red are not as well grouped as ERA5 comparisons seen in blue. Evidence of the small RH MAD in ERA5 is also evident in n Figure 9 since the spread of the data is nearly symmetrical and the extents of the tails are not as large as the plotted NCEP results.

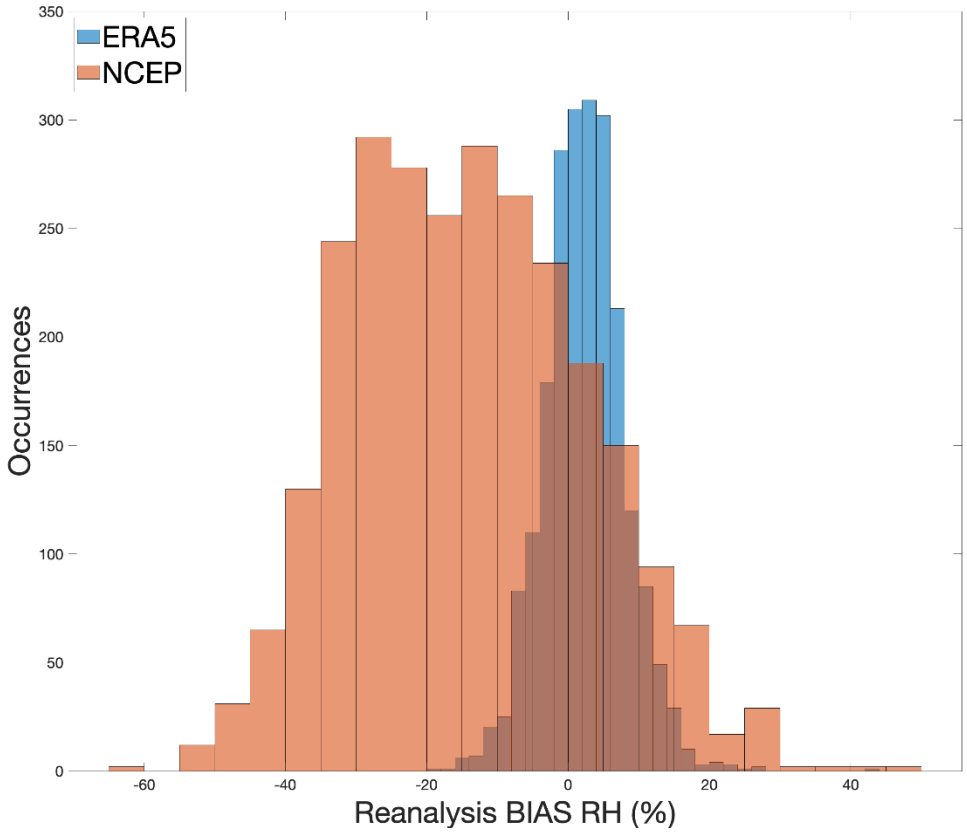

A histogram of the calculated RH differences (Reanalysis minus RO). ERA5 is plotted in blue and NCEP is in red. Abscissa is the percent of BIAS difference and on the ordinate is the number of occurrences. 155067 NCEP vs. RO differences were calculated and 154,372 ERA5 vs. RO.

Figure 9. Guam Composite Reanalysis RH BIAS

The Guam NCEP vs. RO temperature comparison results with similar metrics as the INDOPACOM comparison, as seen in Table 8. Like the IDOPACOM AOI results, Guam has a larger monthly variation in the BIAS in August than INDOPACOM. However, the Guam temperature BIAS in August is the smallest of all months examined, whereas the INDOPACOM BIAS in August was the largest. Guam's monthly negative temperature BIAS is outside the corresponding INDOPACOM BIAS CI for May, July, and August. Guam's composite negative BIAS of -0.19°C is within INDOPACOM's confidence interval of -0.20°C to -0.19°C.

Table 8. Guam - NCEP vs. RO - Temperature °C

	May	June	July	August	Composite
Occurrences	760	593	550	760	2663
BIAS	-0.21	-0.22	-0.20	-0.14	-0.19
BIA CI	-0.27 to -.15	-0.27 to -0.17	-0.25 to -0.16	-0.19 to -0.08	-.22 to -.16
SDD	0.82	0.61	0.57	0.79	0.72
MAD	0.52	0.46	0.43	0.42	0.46
MAD CI	0.47 to .57	0.42 to 0.49	0.39 to 0.46	0.38 to .47	.44 to .48
SDAD	0.67	0.47	0.43	0.68	0.59

Table notes: A Student's t-test was conducted for the monthly and composite BIAS and MAD data sets. All t-test resulted with data being statistically significant and P-value of zero.

The number of outliers present is much more extensive for the INDOPACOM AOI than in Guam, as seen in Figure 7 and Figure 10. These two figures demonstrate how the interquartile ranges, monthly variation, and negative temperature BIAS comparisons in Guam exemplify the INDOPACOM NCEP vs. RO temperature results. The temperature BIAS and MAD results for the Guam and INDOPOACOM NCEP vs. RO comparisons differences are less than half a degree. However, none of the MAD CI overlap for the INDOPACOM and Guam temperature comparisons with NCEP. This result suggests Guam has a significant temperature MAD.

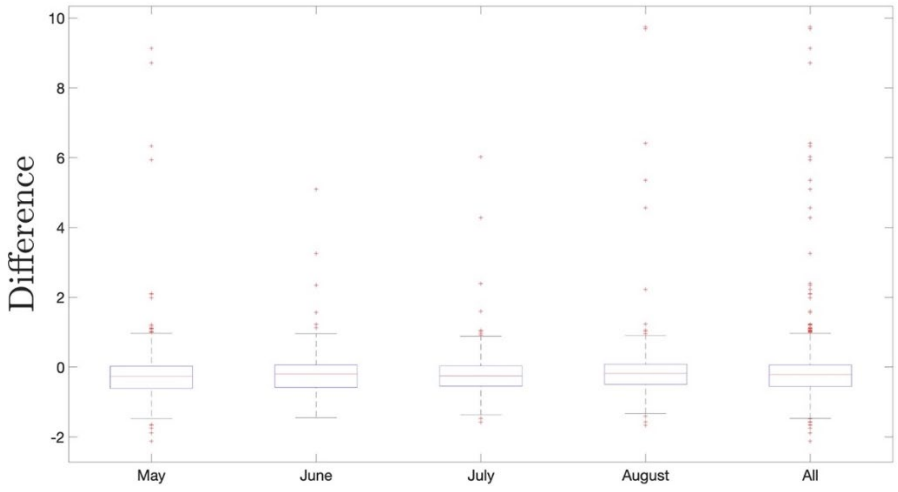

Figure 10. Guam - NCEP vs. RO - Temperature °C Distribution Spread

The Guam ERA5 vs. RO comparisons with temperature results are in Table 9. Unlike the NCEP Guam temperature analysis, the ERA5 temperature differences with RO are all within the BIAS CI and MAE CI of the ERA5 INDOPACOM results. Therefore, they are not statistically significant. The scope of the magnitude of values found in Table 9 is outside the scope of this study.

Table 9. Guam - ERA5 vs. RO - Temperature °C

	May	June	July	August	Composite
Occurrences	616	471	471	596	2154
BIAS	2.23	2.31	2.31	2.32	2.27
BIA CI	2.17 to 2.99	2.27 to 2.35	2.27to 2.35	2.26 to 2.38	2.25 to 2.30
SDD	0.81	0.48	0.48	0.78	0.67
MAD	2.23	2.31	2.31	2.32	2.27
MAD CI	2.17 to 2.99	2.26 to 2.35	2.26 to 2.35	2.26 to 2.38	2.25 to 2.30
SDAD	0.81	0.48	0.48	0.78	0.67

Table notes: A Student's t-test was conducted for the monthly and composite BIAS and MAD data sets. All t-test resulted with data being statistically significant and P-value of zero.

3. Conditional Quantile RH Analysis

The composite results for the INDOPACOM and Guam reanalysis comparisons vs. RO alone do not capture in what situations the model may have been negatively or positively biased. The SDD results from the reanalysis vs. RO comparisons indicate errors can be largely positive or negative. Therefore, a quantile plot is used to demonstrate when the reanalysis and RO differences of RH are occurring, as seen in Figure 11-12 and Figure 14-15. To construct the conditional quantile plot, the mean RH from 850–500mb for each NCEP profile was grouped with its associated RO value. Next, the reanalysis values are sorted numerically and grouped by 5% increments of RH outputs, totaling 20 bins. For each bin of RH outputs, a difference from the reanalysis and RO is calculated along with the mean and the associated percentiles 2.5, 25, 50, 75, and 97.5 (Wilks 2006).

The solid, bolded black line in Figure 11-12 corresponds with zero difference between reanalysis and RO. Figure 11 and Figure 14h have the reanalysis RH percentage values are on the abscissa and Figure 12 and Figure 15 have RO RH (%) values plotted on the abscissa. All quantile figures have the reanalysis minus the RO RH differences on the ordinate. the RO differences from the reanalysis are on the ordinate.

Value in Figure 11 that are below zero indicate a reanalysis dry bias relative to RO and values above zero occur when the reanalysis is "wet" compared to RO observations. Therefore, Figure 11 shows NCEP is consistently drier than RO when its RH is below 62% and wetter than RO indicates when its RH is above 62%. This finding is extremely important because it provides more information on the dry -3.64% RH composite BIAS in the NCEP vs. RO comparison in INDOPACOM. Essentially, when the modeled environment is moist, the reanalysis is too moist and when the model output is dry, it is too dry. While moisture is abundant in the INDPACOM AOI, Figure 11 demonstrates the uncertainty of NCEP's ability to capture the amount of RH in the 850–500mb section of the atmosphere. The spread of the 25th and 75th percentiles decrease as the RH values increases for both NCEP and ERA5 results in Figure 11.

The mean difference of the ERA5 RH results in Figure 11 are primarily greater than zero, and this also explains the magnitude of the positive BIAS calculated in the ERA5 vs. RO comparisons in INDOPACOM. The median ERA5 plotted values (dashed purple line) in Figure 11 are between 0% and 6% when the ERA5 RH < 90%. The composite BIAS values are incomplete without the quantile plots. ERA5 is wet compared to RO RH values in INDOPACOM, but the composite BIAS value considered by itself does not convey how the BIAS changes as the model state or atmospheric thermodynamic state changes.

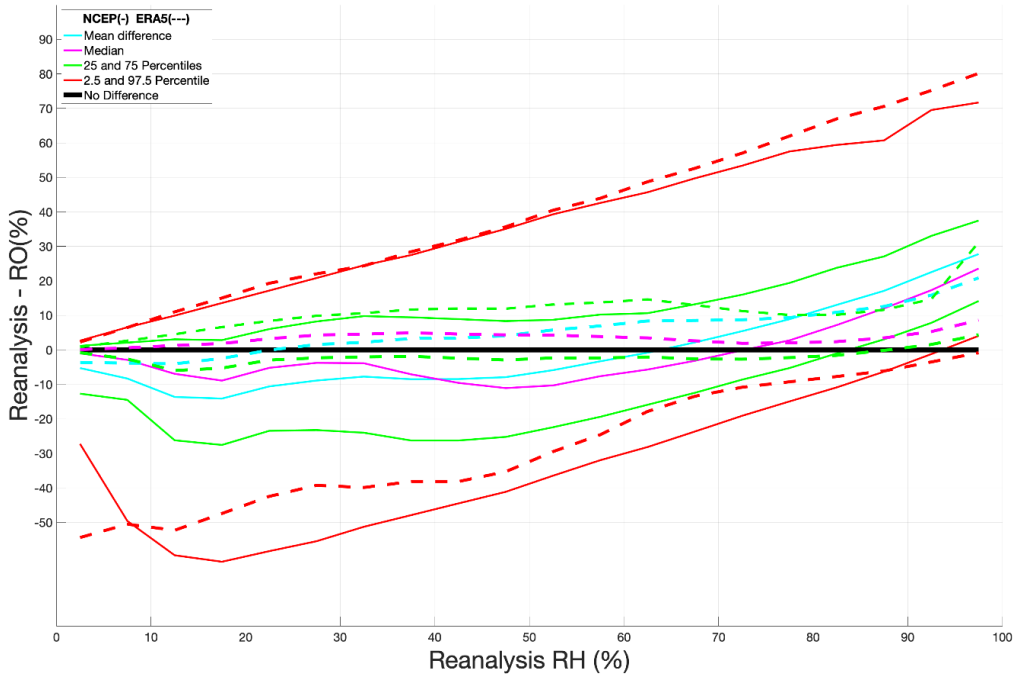

Reanalysis RH (%) values are on the abscissa. The difference (Reanalysis - RO) is on the ordinate. Bold black line denotes no difference from the reanalysis vs. RO comparison. Blue line indicates the average difference. The magenta line is the median or 50th percentile difference. The green line is the 25th and 75th percentiles. The red line is the 2.5 and 97.5 percentile differences. The solid lines represent NCEP values and hashed lines are associated with ERA5 values.

Figure 11. INDOPACOM - Reanalysis vs. RO RH (%) Composite Quantiles

Figure 12 depicts the distributions of differences between reanalysis and RO RH as a function of RH as indicated by RO. This figure illustrates how NCEP and ERA5 behave as moisture concentration in the atmosphere changes. When RO RH values are low, the reanalysis tends to produce a much moister environment and vice versa at high RH values. For example, when RO indicates a RH of 20%, the median ERA5 RH is about 40%. The mean and median differences between RO and ERA5 occur between 60 and 70% RH, where the dashed magenta line crosses the black line. NCEP shows similar behavior at low RO RH; however, its mean and median difference compared to RO occurs for observed RO RH between 40 and 50%.

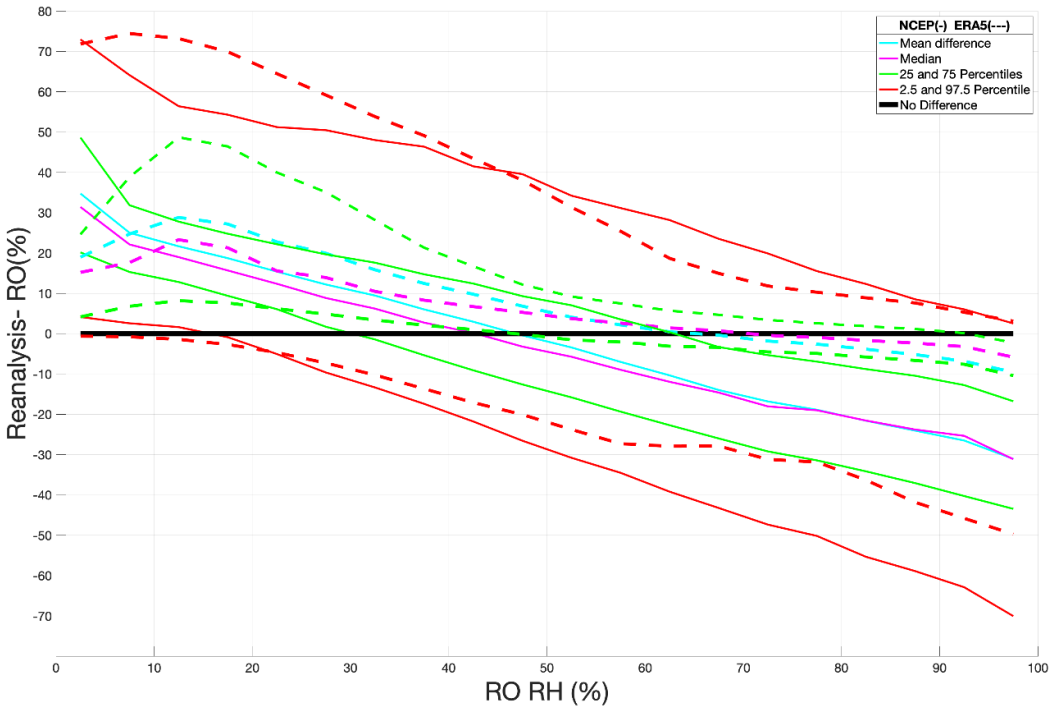

RO RH (%) values are on the abscissa. The difference (Reanalysis - RO) is on the ordinate. Bold black line denotes no difference from the reanalysis vs. RO comparison. Blue line indicates the average difference. The magenta line is the median or 50th percentile difference. The green line is the 25th and 75th percentiles. The red line is the 2.5 and 97.5 percentile differences. The solid lines represent NCEP values and hashed lines are associated with ERA5 values.

Figure 12. INDOPACOM - RO vs. Reanalysis RH (%) Composite Quantiles

To complete the picture of moisture uncertainty in INDOPACOM Figure 13 is provided. In Figure 13 the number of profiles for the reanalysis and RO observations are plotted against RH (%). Here we see ERA5 and RO are fairly aligned. At low RH values, RO has more recorded profiles than ERA5 and several conclusions can be drawn from this finding. Previous studies have demonstrated RO's ability to capture moisture accurately in dry conditions(e.g. Ho et al. 2020b,a, 2007). However, the known issue of RO possessing a negative refractivity bias near the PBL may also be causing more RO profiles to appear at low RH than ERA5. Because RO is assimilated into ERA5 (Hersbach et al. 2020), it is unsurprising to see the similarities in Figure 13. The BIAS of NCEP is evident in Figure 13, with the majority of profiles reporting and average RH near 40%. The ERA5 and RO peaks near 70% RH is more suggestive of the expected environment in INDOPACOM

because this RH is close to a “critical value” to which the atmospheric state tends to evolve (Wolding et al. 2020).

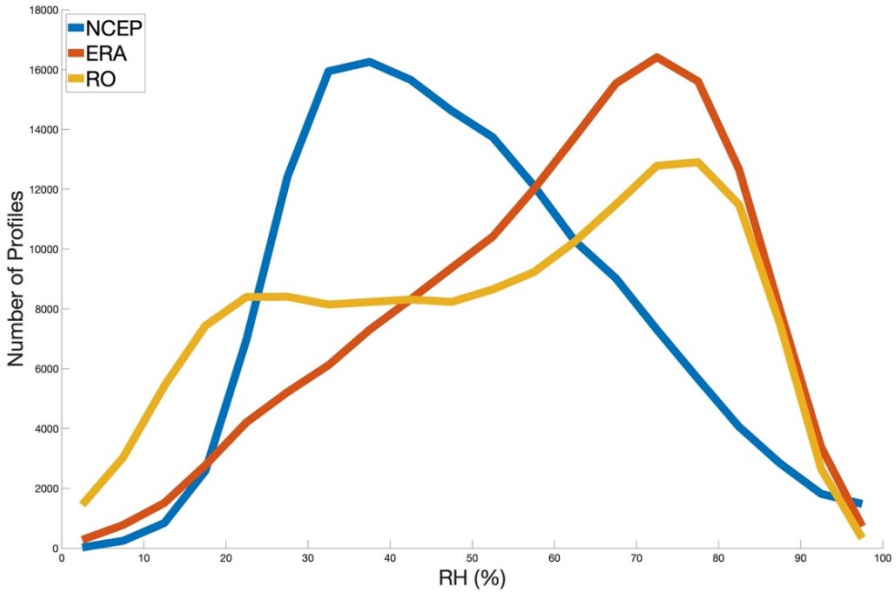

Frequencies of reanalysis and RO RH (%) values have a bin size of 5% and the associated number profiles is on the ordinate.

Figure 13. The Frequency of RH (%) Output Values of Reanalysis and RO in INDOPACOM

The Guam conditional quantile plot with the reanalysis RH on the abscissa is seen in Figure 14. The INDOPACOM and Guam quantile plots show NCEP RH is continuously less-than the corresponding RO value when the NCEP RH is low, indicating that low RH conditions in the NCEP tend to be unrealistically dry. This is evident as the mean difference line is below the black line. The minimum differences (crossing of the no difference line) occurs 62% in Figure 11 for INDOOPACOM AOI and near 68% in Figure 14 for Guam. This corresponds with the Guam NCEP vs. RO RH values having a larger RH BIAS than seen in the INDOPACOM comparisons. The dry BIAS in NCEP appears to have a consistently large difference greater than 15 between 18–48% RH. The 25th and 75th percentiles are continuously dry for NCEP until 65% RH. In the Guam NCEP vs. RO

comparison Figure 14 displays a large dry BIAS. The magnitude of the NCEP mean and median lines in Figure 14 at RH greater than 80% show NCEP also has a large moist BIAS.

When analyzing the ERA5 values in Figure 14, the 2.42% wet BIAS and 5.7% SDD from Table 7 comparison with RO is evident. The mean and median of ERA5 remain almost entirely above the no difference line, indicating a wet bias. Additionally, the 25th and 75th percentiles follow the mean and median lines consistently showing the spread of the difference is small in magnitude which relates to low composite SDD value of 5.7% in the ERA5 Guam comparison.

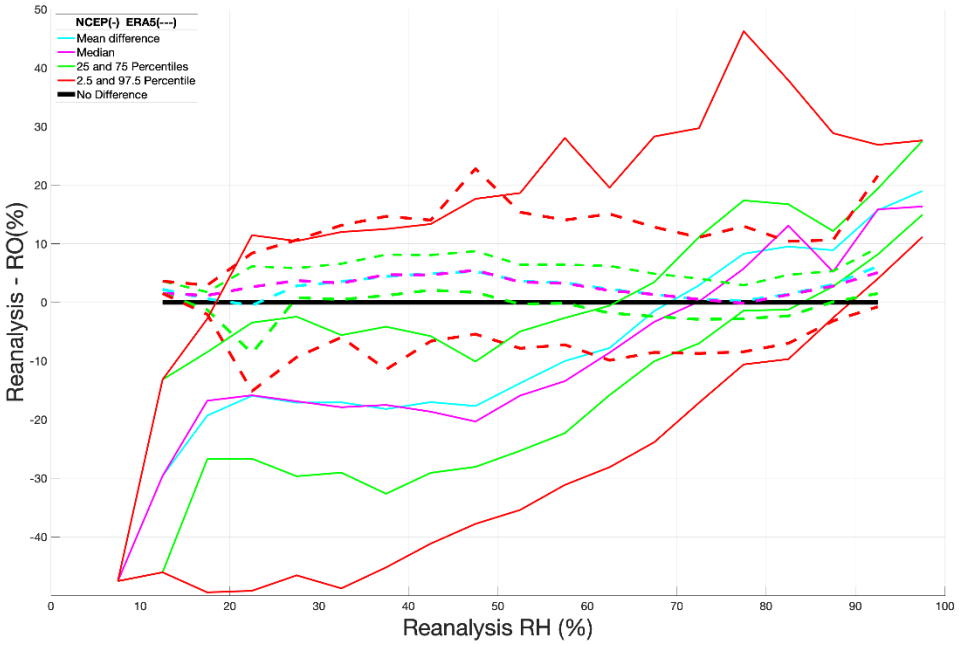

Reanalysis RH (%) values are on the abscissa. The difference (Reanalysis - RO) is on the ordinate. Bold black line denotes no difference from the reanalysis vs. RO comparison. Blue line indicates the average difference. The magenta line is the median or 50th percentile difference. The green line is the 25th and 75th percentiles. The red line is the 2.5 and 97.5 percentile differences. The solid lines represent NCEP values and hashed lines are associated with ERA5 values.

Figure 14. Guam - Reanalysis vs. RO RH (%) Composite Quantiles

RO RH is on the abscissa in the Guam composite quantile plot seen in Figure 15. When RO is reports RH greater than 35% the NCEP output becomes increasingly negatively biased, implying an output that is much drier than the recorded RO observation.

The ERA5 mean and median lines in Figure 15 show the greatest difference occurs when RO is reporting low RH values. When this occurs, ERA5 has a wet BIAS.

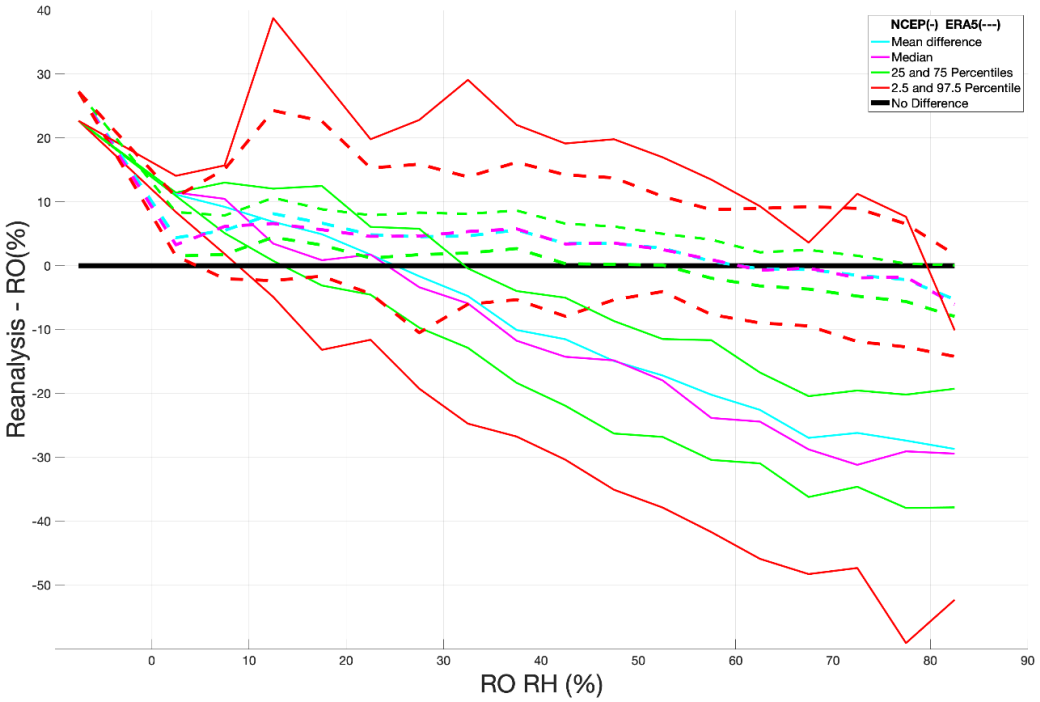

RO RH (%) values are on the abscissa. The difference (Reanalysis - RO) is on the ordinate. Bold black line denotes no difference from the reanalysis vs. RO comparison. Blue line indicates the average difference. The magenta line is the median or 50th percentile difference. The green line is the 25th and 75th percentiles. The red line is the 2.5 and 97.5 percentile differences.

Figure 15. Guam - RO vs. Reanalysis RH (%) Composite Quantiles

Figure 16 shows a greater alignment than Figure 13 with the number of reported RH values from ERA5 and RO. It appears ERA5 and RO are capturing an atmosphere in Guam that are fairly congruent to each other; however, there were not enough samples of either in Guam to accurately assess statistical significance. The differences in the lower RH values between ERA5 and RH in Figure 16 may be highlighting the known negative bias of RO near the PBL (Ho et al. 2020a). The dry BIAS discovered in the NCEP

comparisons with RO is apparent in Figure 16. The lack of RH values greater than 60% presents evidence that errors exist in the NCEP cumulus parameterizations.

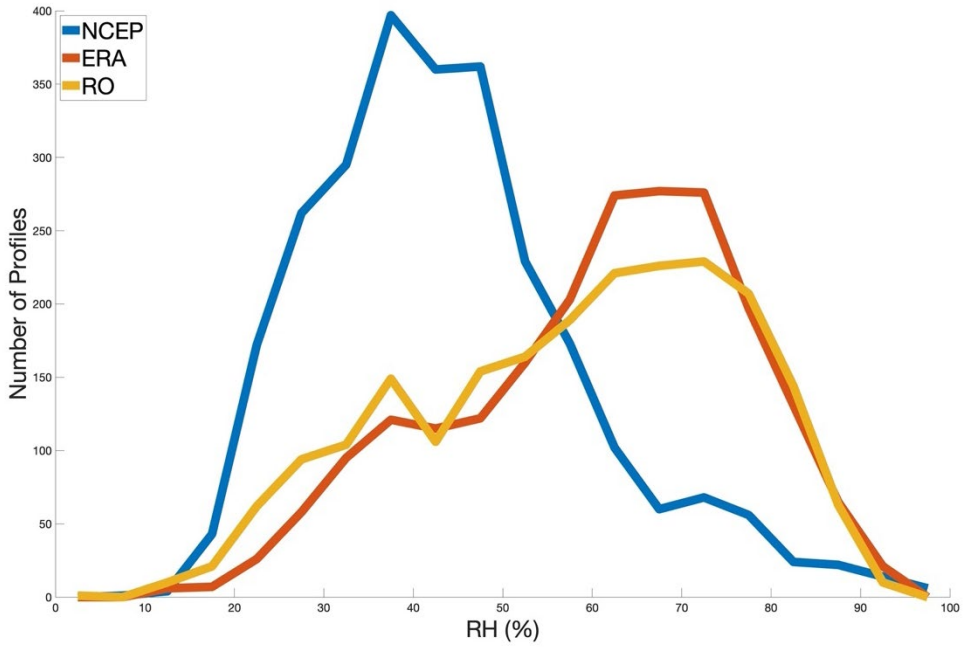

Frequencies of reanalysis and RO RH (%) values have a bin size of 5% and the associated number profiles is on the ordinate.

Figure 16. The Frequency of RH (%) Output Values of Reanalysis and RO in Guam

B. NCEP VS. RADIOSONDE COMPARISONS

1. GUAM NCEP vs. Radiosonde Comparisons

NCEP and Radiosonde were compared to demonstrate the uncertainty of RH and temperature with a trusted and well-respected observation method of launching weather balloons. In the radiosonde comparison, July has the greatest RH BIAS is -18.40%, as seen in Table 10. The RH composite BIAS is smaller in the radiosonde comparison than in the Guam NCEP vs. RO comparison, but the occurrences were only 244 compared to 2663. However, in the INDOPACOM RH BIAS in the NCEP vs. RO comparison is -3.64%, less than the Radiosonde comparison result. When examining the INDOPOACOM NCEP vs. RO, Guam NCEP vs. RO, and NCEP vs. Radiosonde RH comparisons, all result with a

negative monthly and composite BIAS. In these three RH NCEP RH comparisons, the composite results CI did not overlap, suggesting these differences are significant.

The RH MAE for the three cases (INDOPACOM NCEP vs. RO, Guam NCEP vs. RO, and Guam NCEP vs. Radiosonde) result with similar monthly MAE and SDAD for May and June as seen in Table 2, Table 6, and Table 10. May and June, the RH MAE for the NCEP vs. RO comparison is within the CI of the NCEP vs. Radiosonde comparison. The composite MAE for NCEP vs. RO is just outside the NCEP vs. Radiosonde RH MAE confidence interval by 1%. The INDOPACOM RH NCEP vs. RO MAE are in the confidence interval or just 1% outside of the NCEP vs. Radiosonde RH MAE CI. The overlapping CI mention above gives confidence in RO ability to capture similar RH differences as the radiosonde.

The range of the monthly MAE for the three cases (INDOAPCOM NCEP vs. RO, Guam NCEP vs. RO, and NCEP vs. Radiosonde) varies with Guam NCEP vs. RO having the largest monthly MAE range of 14.77% (11.13% to 25.9%). The INDOPACOM has the smallest RH monthly range MAE of 4.11%, but it also has the most data points: 155,067. Looking at the RH SDAD for the three cases, we see less monthly variability. The range of the monthly SDAD for all comparisons was from 9.57% to 14.98%. Therefore, the variation of MAE was similar for all scenarios. The RO comparisons with NCEP in INDOPACOM and Guam result with MAE values either within the confidence interval of the NCEP vs. Radiosonde comparison or within 2% of the interval.

Table 10. Guam - NCEP vs. Radiosonde - RH (%)

	May	June	July	August	Composite
Occurrences	62	60	60	62	244
BIAS	-1.2	-3.81	-18.40	-14.47	-9.45
BIAS CI	-5.73 to 3.13	-8.49 to 0.85	-21.18 to -15.63	-17.97 to -10.97	-11.58 to -7.31
SDD	17.80	18.09	10.74	13.77	16.91
MAE	14.01	13.75	18.59	17.49	15.96
MAE CI	11.25 to 16.78	10.59 to 16.91	15.91 to 21.28	15.06 to 19.92	14.58 to 17.34

	May	June	July	August	Composite
SDAD	10.90	12.24	10.40	9.57	10.95

Table notes: A Student's t-test was conducted for the monthly and composite BIAS and MAE data sets. The t-test for May and June were not statistically significant with P-values of .59 and .11. The remaining t-test resulted with data being statistically significant and P-value of zero.

The temperature comparisons of the three cases mentioned thus far result with a negative BIAS. Therefore, NCEP temperature outputs are slightly less than the RO and radiosonde observations. The most prominent temperature BIAS for the NCEP comparisons is with the radiosonde profiles in May and June with -1.18°C and -1.14°C, as seen in Table 11. These monthly BIAS increase the composite BIAS to -0.71°C. This is more than double the composite temperature BIAS of the NCEP vs. RO comparisons in INDOPACOM and Guam. The RO temperature comparison in the INDOPACOM composite BIAS is only -.2°C and -.19°C in the Guam comparison. The composite SDD for NCEP vs. radiosonde is 1.41°C. This is the most significant temperature composite SDD as there is no overlap in the corresponding CI. The SDD for NCEP vs. RO in the INDOPACOM are 1.04°C and 0.72°C in Guam.

A goal of the NCEP model is to construct the most accurate representation of the atmosphere, but the largest BIAS and SDD are seen in the radiosonde comparison. Departures from observations are inevitable as the reanalysis assimilates data into a grid. The radiosonde is one of many data points injected into the reanalysis. However, since the greatest temperature departure is seen in the radiosonde comparison, it raises the question of the weight of the observation or the validity of the model dynamics and physics that yield the NCEP output.

The Guam NCEP vs. Radiosonde also had the largest composite temperature MAE of 1.27°C and SDAD of 0.93°C as seen in Table 11. The NCEP vs. RO temperature comparison in INDOPACOM and Guam monthly MAE values had a range of 0.24°C (0.64 °C to 0.88°C) and 0.1°C (0.42°C to 0.52°C) with SDAD range of 0.22°C (0.68°C to 0.90°C) and 0.25°C (0.43°C to 0.68°C), respectively. The MAE for the RO comparisons with NCEP is outside the MAE CI for the NCEP vs. Radiosonde comparison. The Guam NCEP vs. Radiosonde had large temperature monthly MAE and SDAD ranges of 0.56°C

(1.03°C to 1.59°C) and 0.35°C (0.76°C to 1.11°C). The large temperature MAE ranges of the NCEP vs. Radiosonde comparison support the pronounced calculated temperature BIAS in the NCEP vs. Radiosonde comparison.

Table 11. Guam - NCEP vs. Radiosonde - Temperature °C

	May	June	July	August	Composite
Occurrences	62	60	60	62	244
BIAS	-1.18	-1.14	-0.16	-0.34	-0.71
BIAS CI	-1.58 to -0.78	-1.43 to -0.83	-.51 to 0.19	-0.66 to -0.03	-0.88 to -0.53
SDD	1.55	1.17	1.37	1.24	1.41
MAE	1.59	1.32	1.13	1.03	1.27
MAE CI	1.31 to 1.88	1.08 to 1.57	0.92 to 1.33	0.83 to 1.23	1.15 to 1.39
SDAD	1.11	0.95	0.79	0.76	0.93

Table notes: A Student's t-test was conducted for the monthly and composite BIAS and MAE data sets. July BIAS is not statistically significant and result with a P-value of .37. August has a P-value of .03. P-values not mentioned are zero.

C. RADIOSONDE VS. RO COMPARISONS

A Radiosonde vs. RO RH and temperature comparison was conducted to accurately assess RO's ability to capture the moisture concentration in the atmosphere. The most significant limitation to this inspection is the number of occurrences, 50. The comparison was undertaken only when the RO profiles were within 110km of the radiosonde location. 110km was selected because the NCEP grid point closest to the radiosonde was 111 km. Because the Student's t-test and CI calculations include the sample size, the small sample size in the Radiosonde vs. RO comparisons is a considerable factor. Inferences from the results are taken with caution.

1. GUAM Radiosonde vs. RO Comparisons

The results of the Guam Radiosonde vs. RO RH comparison are listed in Table 12. Here we see a slight positive composite BIAS of 0.1% The sizeable positive RH BIAS in

May significantly contributes to the composite calculation because of its magnitude and the number of occurrences. The composite RH BIAS is 0.10%, and this is the smallest BIAS of all the comparison. However, if the May was reduced, the composite BIAS is similar to the INDOPACOM NCEP vs. RO BIAS value of -3.64%. The student t-test BIAS was not statistically significant.

Table 12. Guam - Radiosonde vs. RO - RH (%)

	May	June	July	August	Composite
Occurrences	18	10	9	13	50
BIAS	3.70	-3.06	-2.13	-0.90	0.10
BIAS CI	-0.61 to 8.02	-9.45 to 3.33	-6.14 to 1.92	-6.29 to 4.45	-2.32 to 2.52
BIAS P-value	.08755	.3069995	.2616931	.7155988	.93256
SDD	8.67	8.93	5.26	8.87	8.51
MAE	7.35	7.43	4.99	7.54	6.99
MAE CI	4.52 to 10.18	3.58 to 11.27	3.30 to 6.64	4.99 to 10.12	5.64 to 8.34
SDAD	5.69	5.37	2.18	4.23	4.75

Table note: Table notes: A Student's t-test was conducted for the monthly and composite BIAS and MAE data sets. All of the BIAS t-test are not statistically significant.

The monthly and composite SDD and SDAD for the Radiosonde vs. RO RH comparison are the smallest in magnitudes of all the aforementioned comparisons. The composite values for each of the comparisons are listed in Table 13. Although the Radiosonde vs. RO comparisons is comprised of a small sample size, the values from Table 12 and Table 13 shows RO's ability to accurately depict the moisture with minimal BIAS and MAE with the "known truth" radiosonde values.

Table 13. RH (%) Composite Comparisons

	INDOPACOM	Guam		
Comparison	NCEP vs. RO	NCEP vs. RO	NCEP vs. Radiosonde	Radiosonde vs. RO
Occurrences	155067	2663	244	50
BIAS	-3.64	-14.02	-9.45	.10

	INDOPACOM	Guam		
SDD	22.22	16.63	16.91	8.51
MAD	17.93	18.07	15.96	6.99
SDAD	13.62	12.12	10.95	4.75

The results of the temperature comparison of Radiosonde vs. RO over Guam are found in Table 14. Here we see a composite BIAS of 0.38°C and monthly BIAS range from -0.62°C to 1.23°C. With the composite value of 0.38°C, we may infer RO temperature value is less than the observed radiosonde value. Unlike the previous caparisons for temperature, these monthly values fluctuate from positive to negative. However, the number of occurrences per month is low and with the exception of May the BIAS were not statistically significant. The composite SDD for this temperature comparison is identical to the NCEP vs. radiosonde comparison. Therefore, the distribution spared of the temperature profiles differences are similar. Table 4, Table 8, and Table 11 all show comparisons with NCEP, and every monthly temperature BIAS is negative. NCEP continuously produces an output with a lower temperature than the radiosonde and RO observations.

Table 14. Guam - Radiosonde vs. RO - Temperature °C

Occurrences	May	June	July	August	Composite
Occurrences	18	10	9	13	50
BIAS	1.23	0.26	-0.62	-0.03	0.38
BIAS CI	0.57 to 1.89	-0.28 to 0.81	-1.86 to 0.64	-0.72 to 0.68	-0.17 to .78
BIAS P-value	.001	.3086	.295	0.9587	.0607
SDD	1.3	0.77	1.61	1.17	1.41
MAE	1.48	0.62	1.11	0.80	1.06
MAE CI	.96 to 1.99	0.26 to .97	0.13 to 2.11	0.29 to 1.29	0.78 to 1.34
SDAD	1.03	0.49	1.28	0.81	0.98

Table note: Table notes: A Student's t-test was conducted for the monthly and composite BIAS and MAE data sets. June, July, August, and Composite BIAS are not statistically significant.

D. NORMALIZED COMPOSITE COMPARISONS

Normalized RH and temperature composite BIAS and MAD results from each comparison are listed in Table 15. The NORM BIAS and NORM MAD values for RH, reveal NCEP has a greater difference than temperature from the observed RO and radiosonde observations. The difference in NORM BIAS and NORM MAD for temperature for each comparison is less than 1%. The Radiosonde vs. RO comparison results with the smallest RH NORM BIAS and NORM MAD with values of 0.20% and 14% respectively. The normalized results for the Radiosonde vs. RO comparison further validates the idea that RO is a more accurate representation of the true atmospheric state than reanalysis. The NORM MAD for each comparison with NCEP were fairly aligned with values ranging from 29–31%. The RH and temperature NORM BIAS and NORM MAD results confirms our hypotheses concluding NCEP uncertainty with moisture exceeds the uncertainties associated with temperature.

Table 15. Normalized Composite Comparisons (%)

	INDOPACOM	Guam		
Comparison	NCEP vs. RO	NCEP vs. RO	NCEP vs. Radiosonde	Radiosonde vs. RO
Occurrences	155067	2663	244	50
NORM BIAS RH	-7	-23	-18	0.20
NORM MAD RH	32	30	29	14
NORM BIAS TEMP	-0.50	-0.07	-0.25	0.13
NORM MAD TEMP	0.69	0.26	0.45	0.37

E. ML-CAPE COMPARISONS

For each of the NCEP corresponding RO profile a comparison of ML-CAPE, and ML-ECAPE was conducted, seen in Table 16. Only the SDD and SDAD are fairly aligned, and this indicates there is not much difference in the spread of the ML-CAPE and ML-ECAPE differences between INDOPACOM and Guam. However, the results in Table 16 demonstrate the vast amount of uncertainty global models have on capturing the

thermodynamic processing of mesoscale systems. This is clearly seen as the largest sample size has the greatest NORM MAD results exceedingly over 100%. A rigorous determination of sources of these errors and biases is beyond the scope of this work. A likely contributing factor may be attributed to the prevalent negative temperature and RH BIAS results in the NCEP relative to RO and radiosondes in the 850–500 hPa section of the atmosphere, seen in Table 15. The negative RH and temperature BIAS findings correspond to a negative or low bias in virtual temperature aloft. With cooler temperatures aloft, mean-layer unstable parcels would have an associated high positive BIAS in buoyancy in the NCEP profiles. A false positive buoyancy BIAS would then result in the positive ML-CAPE and ML-ECAPE values seen in Table 16.

Table 16. ML-CAPE Composite Comparisons NCEP vs. RO (Jkg^{-1})

	INDOPACOM		GUAM	
	155067		2663	
	ML-CAPE	ML-ECAPE	ML-CAPE	ML-ECAPE
BIAS	337	139	138	99
NORM BIAS	64%	115%	84%	22%
SDD	585	308	503	353
MAD	420	181	402	252
NORM MAD	126%	126%	57%	118%
SDAD	528	285	333	266

F. CM1 SIMULATION OUTPUTS

Our CM1 simulations demonstrate how the middle tropospheric RH uncertainties identified in our analysis may impact the behavior of convection. We ran two simulations: a "control," which used an observed radiosonde profile from August 13, 2020, and a "dry" simulation, where the RH in the 850–500 hPa layer from this sounding was reduced by 15%. In the control profile, the mean RH from 850–500 hPa layer was 87%. The INDOPACOM quantile plot in Figure 11 shows a 17% wet BIAS when NCEP RH is 87%. To show the impact of this wet BIAS, the simulation reduced the control 850–500 hPa RH

by 15%, as seen in Figure 17b. The control simulations depict the dynamical outputs produced by NCEP with a moist BIAS and the reduced simulations portrays the corresponding RO at 87% RH. Figure 18 is time series of the simulation results. Figure 17 displays the control and the reduced RH profiles. Both profiles have nearly identical CAPE and the differences in storm behavior resulting from the differences in these soundings would be difficult to discern from a forecasting perspective. However, the 15% reduced RH in the 850–500 hPa layer results in an increase in entrainment-driven dilution of buoyancy in the dry profile relative to the control profile, which can be seen as a 45% reduction in ECAPE.

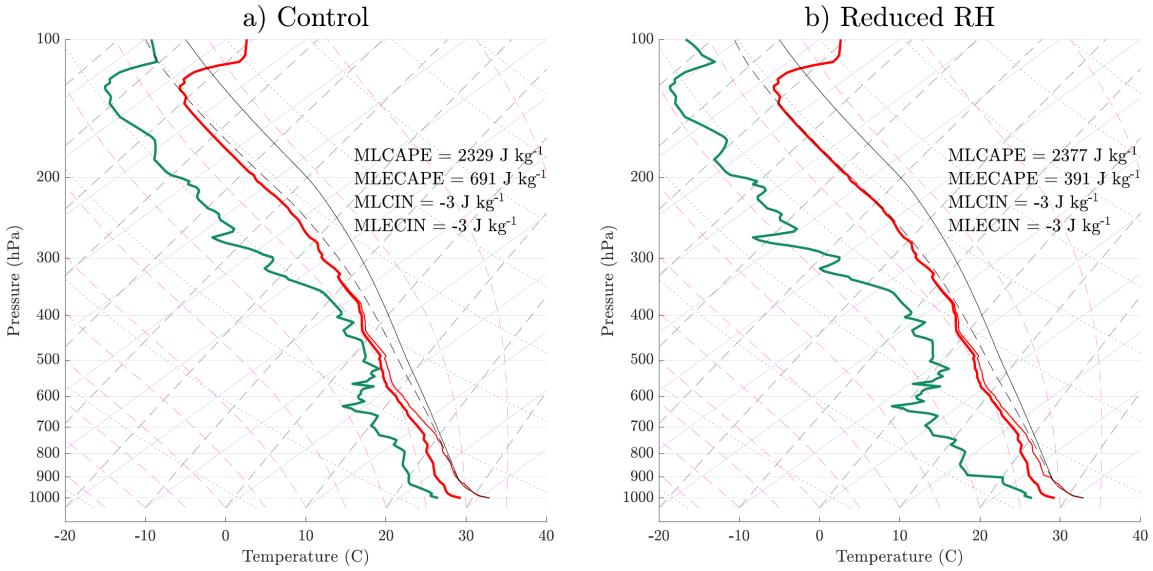

Skew-T diagrams for CM1 input soundings simulations. a) Controlled sounding profile from radiosonde launched at 00Z August 13, 2020 in Guam. b) Profile moisture profile is reduced by 15% in the 850–500 hPa section of the atmosphere. Source: Images created in MATLAB R2020b.

Figure 17. Atmospheric Sounding for CM1 Simulations

In the CM1 simulations, the minimum threshold for defining cloud top heights is set to 3 m/s. Deep moist convection is evident in the controlled simulation as a rapid increase in the depth of updraft between 1 hour and 1.25 hours, with maximum vertical velocities exceeding 50 m/s and updraft of > 3 m/s exceeding 17 km in depth (Fig. 15a, c-d). Convective intensity declined quickly after this initial peak. This rapid peak and decline

in intensity is a common feature of weakly sheared tropical convection, which is often "pulse-like" in nature (e.g., Weisman an Klemp 1982). A similar time evolution of convection is evident in the dry simulation, but with the depth of >3 m s^{-1} updraft only reaching 14 km, and maximum vertical velocities only reaching 30 m s^{-1} -- roughly 45% weaker than that of the control simulation. Figure 18abd shows this difference in max *w* is nearly double for a profile with the same surface-based CAPE, but reduced moisture by 15% in the 850–500 hPa section of atmosphere. Because of the strong *w* in the control profile, cloud heights in Figure 18cf or the controlled profile remain above the reduced RH peak for nearly half an hour. The INDOPACOM NCEP vs. RO RH comparison resulted with monthly MAD ranging from 16.24 % to 20.35% with CI spanning less than 1%. The corresponding Guam RH comparison with NCEP and RO had a larger range from 11.13% to 25.9% and CI spanning less than 2%. This single numerical modeling experiment expresses how a moisture difference of 15% can result in large differences in outcome of convection.

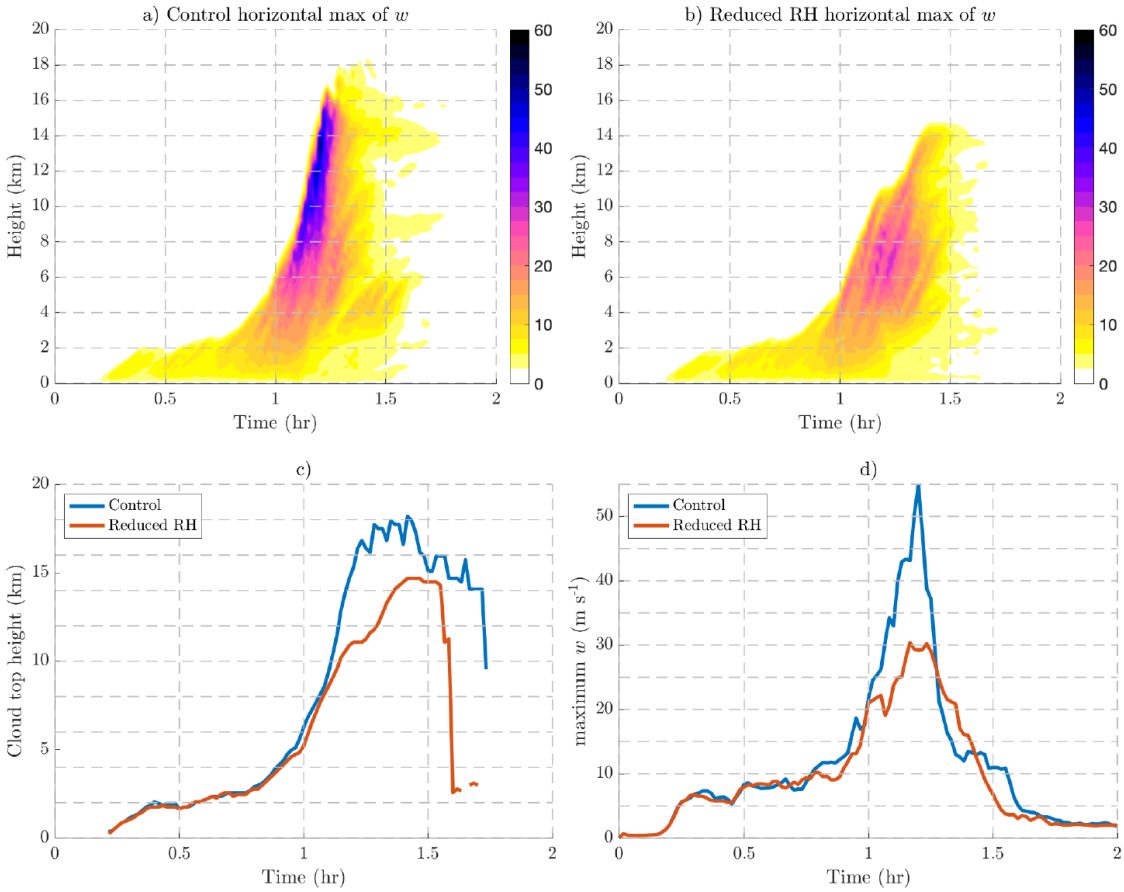

Both the control and reduced RH profiles had identical surface-base CAPE values. The moisture profile of the reduced RH simulation had a 15% moisture reduction in the 850–500 hPa section of the atmosphere. a) Control profile time series of max vertical velocity in color contour with units of (m/s). b) Reduced RH profile time series of max vertical velocity in color contour with units of (m/s). c) Time series of cloud top height (km) for control and reduced RH profiles. d) Time series of maximum vertical velocity (m/s) of control and reduced RH profiles.

Figure 18. CM1 Simulation with a Reduced RH Profile

THIS PAGE INTENTIONALLY LEFT BLANK

IV. CONCLUSION

Accurate portrayal of the horizontal variability in water vapor concentration is critical for numerical models to produce accurate analyses and forecasts of moist convection in the atmosphere. Quantifying how accurately numerical models capture the vertical distribution of water vapor and the impact of this uncertainty on deep moist convection is the focus of this research. Despite the many advances of numerical modeling, accurate representation of how numerous interconnected processes impacts atmospheric water vapor has remained elusive. Atmospheric forecast models will inevitably have a great amount of uncertainty because the atmosphere is described as a nonlinear system which is dependent on initial conditions. Through Lorenz's "chaos theory" it is known that numerical models are very sensitive to the initial conditions and because it is currently impossible to observe the complete atmosphere in a single time in space. This is not possible because of the lack of observations and the atmosphere has processes that are either too small or too fast to be explicitly captured by the current spatial resolution of numerical models. Nevertheless, quantifying the uncertainty of how we depict the atmosphere serves as reason for further research with a metric to improve upon.

With the rapid increase in the usage of satellite-based remote sensing in recent decades, our ability to observe and measure the atmosphere has expanded exponentially. GNSS are constantly transmitting signals towards Earth and due to the nature of the atmosphere, some signals are bent and captured by satellites orbiting in LEO, thus producing RO. This research leverages the recently launched COSMIC-2 satellites which are configured to receive RO to measures the Earth's temperature, pressure, and water vapor content via the collected reflectivity bending angles. The wetPrf2 RO signals are used to measure the uncertainty of water vapor content in middle tropospheric layer spanning from 850–500 hPa. The NCEP R2, reanalysis model is known to provide a comprehensive record of the atmosphere by the blending of model forecast and observation (Kanamitsu et al. 2002). This research has conducted an evaluation of the uncertainty present in NCEP R2 atmospheric profiles through direct comparisons of the atmospheric profiles provided by RO. 155,067 NCEP R2 reanalysis profiles were compared with

corresponding COSMIC RO observations for the IDNOPACOM AOI. A subset of 2663 from the 155,067 profiles were analyzed to quantify the uncertainty for the localized region of Guam. This research results with the following conclusions:

- Moisture is not adequately captured in the NCEP R2 reanalysis, therefore, the NCEP R2 reanalysis is producing atmospheric profiles that do not properly convey convection. Composite results reveal a dry BIAS exists. Condition quantile analysis expand upon dry BIAS and expose evidence of an "all or nothing" behavior in the NCEP R2 cumulus parameterization with RH extremes being over exemplified. In convective environments the NCEP R2 reanalysis is producing environments with much greater RH than observed and vice versa for non-convective environments.

- NORM BIAS and NORM MAD values for RH and temperature reveal NCEP R2 has more uncertainty in moisture profiles than in temperature.

- The NCEP R2 comparisons with RO result with BIAS CI for INDOPACOM and Guam that do not overlap. This result suggests statistical significance, but it cannot be explicitly stated because of Guam's sample size and the distribution of the differences.

- NORM BIAS and NORM MAD results for ML-CAPE and MLE-CAPE quantify the NCEP R2's reanalysis inability to capture atmospheric profiles for mesoscale systems.

- ERA5 benefits from assimilating RO. The ERA5 analysis with RO demonstrates a greater correspondence than the NCEP R2 comparison with RO. ERA5 profiles have less moisture uncertainty than NCEP R2 reanalysis.

The concentration of water vapor plays a critical role in global circulation patterns via the vertical distribution of heat via convective transport, and through absorption and emission of radiation (Arakawa 2004). On a localized and forecasting perspective, the amount of water vapor present may determine if moist convection occurs. The NCEP R2

reanalysis does not have the horizontal or temporal resolutions to resolve deep moist convection.

The CM1 simulations explore the NCEP R2's reanalysis limitations and demonstrate the impact of moisture uncertainty. Reducing the moisture by 15% in the middle troposphere has a substantial impact on determining if deep moist convection occurs. Both of the CM1 simulations produced deep moist convection, but the difference in the severity was substantial. CM1 simulations resulted with a nearly double difference in the max vertical velocity when the RH was reduced by 15%. Capturing the forecast intensity of convection is paramount for naval operations and these simulations demonstrate how a reduction in moisture could dramatically impact storms. From a global weather and climate prediction aspect, the differences in the CM1 simulations results show moisture differences may impact our ability to accurately capture the influence of convection on global circulation patterns.

The INDOPACOM is an expansive operating space for the U.S. Navy and this study only captures the localized differences in RH profiles for NCEP R2 reanalysis in Guam. Results from this study can be leveraged to explore and expose other localized areas where differences in RH may impact Navy operations. Because reanalysis models such as NCEP R2 reanalysis have a constant physics, dynamics, and data assimilation system, RO observations from the recent COSMIC-2 launch are not incorporated into the analysis. The updated CSFR reanalysis model does incorporate these RO observations (Saha et al. 2010). A further analysis could be conducted to evaluate if CFSR benefits from RO similarly to ERA5. An analysis between ERA5, NCEP R2, and CFSR could further assess the uncertainty of moisture in the atmosphere. Lastly, further research can expand upon the results of this thesis to tailor cumulus parameterizations and forecast ensembles to encapsulate the uncertainty found in this study.

THIS PAGE INTENTIONALLY LEFT BLANK

LIST OF REFERENCES

Ackerman, Steven and Knox, J., 2015: *Meteorology Understanding the Atmosphere*. 4th ed. Jones and Bartlett Learning, LLC, an Ascend Learning Company, 575 pp.

American Meteorological Society, 2012a: Moist convection - Glossary of Meteorology. https://glossary.ametsoc.org/wiki/Moist_convection (Accessed September 7, 2021).

——, 2012b: Water vapor - Glossary of Meteorology. https://glossary.ametsoc.org/wiki/Water_vapor (Accessed September 7, 2021).

Arakawa, A., 2004: The Cumulus Parameterization Problem: Past, Present, and Future. *J. Climate*, **17**, 2493–2525, https://doi.org/10.1175/1520-0442(2004)017<2493:RATCPP>2.0.CO;2.

Bengtsson, L., and Coauthors, 2003: The Use of GPS Measurements for Water Vapor Determination. *Bull. Amer. Meteor. Soc.*, **84**, 1249–1258, https://doi.org/10.1175/BAMS-84-9-1249.

Bevis, M., S. Businger, T. A. Herring, C. Rocken, R. A. Anthes, and R. H. Ware, 1992: GPS meteorology: Remote sensing of atmospheric water vapor using the global positioning system. *J. Geophys. Res.*, **97**, 15787, https://doi.org/10.1029/92JD01517.

Biondi, R., T. Neubert, S. Syndergaard, and J. K. Nielsen, 2011: Radio occultation bending angle anomalies during tropical cyclones. *Atmos. Meas. Tech.*, **4**, 1053–1060, https://doi.org/10.5194/amt-4-1053-2011.

Bryan, George H. 2011: CM1: Frequently Asked Questions. *Answers to Frequently Asked Questions about CM1*,. https://www2.mmm.ucar.edu/people/bryan/cm1/faq.html (Accessed November 7, 2020).

CDAAC 4.7, 2020: CDAAC: COSMIC Data Analysis and Archive Center - CDAAC Description. *CDAAC File Formats wetPrf*,. https://cdaac-www.cosmic.ucar.edu/cdaac/cgi_bin/fileFormats.cgi?type=wetPrf (Accessed August 8, 2020).

Derbyshire, S. H., I. Beau, P. Bechtold, J.-Y. Grandpeix, J.-M. Piriou, J.-L. Redelsperger, and P. M. M. Soares, 2004: Sensitivity of moist convection to environmental humidity. *Quarterly Journal of the Royal Meteorological Society*, **130**, 3055–3079, https://doi.org/10.1256/qj.03.130.

Hersbach, H., and Coauthors, 2020: The ERA5 global reanalysis. *Q.J.R. Meteorol. Soc.*, **146**, 1999–2049, https://doi.org/10.1002/qj.3803.

Hersbach, H., Bell, B., Berrisford, P., Biavati, G., Horányi, A., Muñoz Sabater, J., Nicolas, J., Peubey, C., Radu, R., Rozum, I., Schepers, D., Simmons, A., Soci, C., Dee, D., Thépaut, J-N. (2018): ERA5 hourly data on pressure levels from 1979 to present. Copernicus Climate Change Service (C3S) Climate Data Store (CDS). (Accessed on < 26-NOV-2021 >), 10.24381/cds.bd0915c6

Held, I. M., and B. J. Soden, 2006: Robust Responses of the Hydrological Cycle to Global Warming. *Journal of Climate*, **19**, 5686–5699, https://doi.org/10.1175/JCLI3990.1.

Ho, S., X. Zhou, Y.-H. Kuo, D. Hunt, and J. Wang, 2010: Global Evaluation of Radiosonde Water Vapor Systematic Biases using GPS Radio Occultation from COSMIC and ECMWF Analysis. *Remote Sensing*, **2**, 1320–1330, https://doi.org/10.3390/rs2051320.

——, and Coauthors, 2020a: The COSMIC/FORMOSAT-3 Radio Occultation Mission after 12 Years: Accomplishments, Remaining Challenges, and Potential Impacts of COSMIC-2. *Bulletin of the American Meteorological Society*, **101**, E1107–E1136, https://doi.org/10.1175/BAMS-D-18-0290.1.

Ho, S.-P., Y.-H. Kuo, and S. Sokolovskiy, 2007: Improvement of the Temperature and Moisture Retrievals in the Lower Troposphere Using AIRS and GPS Radio Occultation Measurements. *Journal of Atmospheric and Oceanic Technology*, **24**, 1726–1739, https://doi.org/10.1175/JTECH2071.1.

——, and Coauthors, 2020b: Initial Assessment of the COSMIC-2/FORMOSAT-7 Neutral Atmosphere Data Quality in NESDIS/STAR Using In Situ and Satellite Data. *Remote Sensing*, **12**, 4099, https://doi.org/10.3390/rs12244099.

Kanamitsu, M., W. Ebisuzaki, S.-K. Yang, J. J. Hnilo, M. Fiorino, and G. L. Potter, 2002: NCEP-DOE AMIP-II REANALYSIS (R-2). *Bulletin of the American Meteorological Society*, **83**, 14, https://doi.org/10.1175/BAMS-83-11-1631.

Klemp, J. B., and D. R. Durran, 1983: An Upper Boundary Condition Permitting Internal Gravity Wave Radiation in Numerical Mesoscale Models. *Monthly Weather Review*, **111**, 430–444, https://doi-org.libproxy.nps.edu/10.1175/1520-0493(1983)111<0430:AUBCPI>2.0.CO;2.

Kursinski, E. R., G. A. Hajj, J. T. Schofield, R. P. Linfield, and K. R. Hardy, 1997: Observing Earth's atmosphere with radio occultation measurements using the Global Positioning System. *J. Geophys. Res.*, **102**, 23429–23465, https://doi.org/10.1029/97JD01569.

Ligda, M. G. H., 1955: Hurricane Squall Lines. *Bulletin of the American Meteorological Society*, **36**, 340–342, https://doi.org/10.1175/1520-0477-36.7.340.

Mahan, A. T., 1949: The influence of sea power upon history, 1660–1783. Little, Brown,.

Melbourne, W. G., and Coauthors, The Application of Spaceborne GPS to Atmospheric Limb Sounding 1 Glolbal Change Monitoring. 159.

Moncrieff, M. W., and Miller M. J., 1975: The dynamics and simulation of tropical cumulonimbus and squall lines. *Quart. J. Roy. Meteor. Soc.*, **102**, 373–394, https://doi.org/10.1002/qj.49710243208.

Morrison, H., 2017: An Analytic Description of the Structure and Evolution of Growing Deep Cumulus Updrafts. *Journal of the Atmospheric Sciences*, **74**, 809–834, https://doi.org/10.1175/JAS-D-16-0234.1.

Morrison, H., G. Thompson, and V. Tatarskii, 2009a: Impact of Cloud Microphysics on the Development of Trailing Stratiform Precipitation in a Simulated Squall Line: Comparison of One- and Two-Moment Schemes. *Monthly Weather Review*, **137**, 991–1007, https://doi.org/10.1175/2008MWR2556.1.

——, ——, and ——, 2009b: Impact of Cloud Microphysics on the Development of Trailing Stratiform Precipitation in a Simulated Squall Line: Comparison of One- and Two-Moment Schemes. *Monthly Weather Review*, **137**, 991–1007, https://doi.org/10.1175/2008MWR2556.1.

Morrison, H., J. M. Peters, A. C. Varble, W. M. Hannah, and S. E. Giangrande, 2020: Thermal Chains and Entrainment in Cumulus Updrafts. Part I: Theoretical Description. *Journal of the Atmospheric Sciences*, **77**, 3637–3660, https://doi.org/10.1175/JAS-D-19-0243.1.

National Coordination Office for Space-Based Positioning, Navigation, and Timing, GPS.gov: Space Segment. *Space Segment*,. https://www.gps.gov/systems/gps/space/ (Accessed March 25, 2021).

Nowotarski, C. J., J. M. Peters, and J. P. Mulholland, 2020: Evaluating the Effective Inflow Layer of Simulated Supercell Updrafts. *Monthly Weather Review*, **148**, 3507–3532, https://doi.org/10.1175/MWR-D-20-0013.1.

NWS Internet Services Team, 2009: NWS Glossary ML-CAPE. https://forecast.weather.gov/glossary.php?word=ML-CAPE (Accessed November 9, 2021).

Oloman, Larry, 2020: Atmospheric Soundings. *University of Wyoming College of Engineering*,. http://weather.uwyo.edu/upperair/sounding.html (Accessed April 23, 2020).

Peters, J. M., and P. J. Roebber, 2014: Synoptic Control of Heavy-Rain-Producing Convective Training Episodes. *Monthly Weather Review*, **142**, 2464–2482, https://doi.org/10.1175/MWR-D-13-00263.1.

——, C. J. Nowotarski, and H. Morrison, 2019: The Role of Vertical Wind Shear in Modulating Maximum Supercell Updraft Velocities. *Journal of the Atmospheric Sciences*, **76**, 3169–3189, https://doi.org/10.1175/JAS-D-19-0096.1.

——, H. Morrison, C. J. Nowotarski, J. P. Mulholland, and R. L. Thompson, 2020a: A Formula for the Maximum Vertical Velocity in Supercell Updrafts. *Journal of the Atmospheric Sciences*, **77**, 3747–3757, https://doi.org/10.1175/JAS-D-20-0103.1.

——, ——, A. C. Varble, W. M. Hannah, and S. E. Giangrande, 2020b: Thermal Chains and Entrainment in Cumulus Updrafts. Part II: Analysis of Idealized Simulations. *Journal of the Atmospheric Sciences*, **77**, 3661–3681, https://doi.org/10.1175/JAS-D-19-0244.1.

Romps, D. M., 2010: A Direct Measure of Entrainment. *Journal of the Atmospheric Sciences*, **67**, 1908–1927, https://doi.org/10.1175/2010JAS3371.1.

——, and Z. Kuang, 2010: Nature versus Nurture in Shallow Convection. *Journal of the Atmospheric Sciences*, **67**, 1655–1666, https://doi.org/10.1175/2009JAS3307.1.

Saha, S., and Coauthors, 2010: The NCEP Climate Forecast System Reanalysis. *Bull. Amer. Meteor. Soc.*, **91**, 1015–1058, https://doi.org/10.1175/2010BAMS3001.1.

Thorne, P. W., and R. S. Vose, 2010: Reanalyses Suitable for Characterizing Long-Term Trends. *Bull. Amer. Meteor. Soc.*, **91**, 353–362, https://doi.org/10.1175/2009BAMS2858.1.

UCAR, Introduction. https://www.cosmic.ucar.edu/who-we-are/introduction/ (Accessed October 25, 2021).

U.S. Department of Commerce, N., 2020: Archive. https://www.weather.gov/gum/archive (Accessed October 25, 2021).

Wang, S., and A. H. Sobel, 2012: Impact of imposed drying on deep convection in a cloud-resolving model. *Journal of Geophysical Research: Atmospheres*, **117**, https://doi.org/10.1029/2011JD016847.

Weisman, M. L., and J. B. Klemp J. B., 1982: The dependence of numerically simulated convective storms on vertical wind shear and buoyancy. *Monthly Weather Review*, **110**, 504–520, https://doi-org.libproxy.nps.edu/10.1175/1520-0493(1982)110<0504:TDONSC>2.0.CO;2.

Wilks, D. S. 2006: *Statistical methods in the atmospheric sciences*. 2nd ed. Academic Press, 627 pp.

Winning, T. E., Y.-L. Chen, and F. Xie, 2017: Estimation of the marine boundary layer height over the central North Pacific using GPS radio occultation. *Atmospheric Research*, **183**, 362–370, https://doi.org/10.1016/j.atmosres.2016.08.005.

Wolding, B., J. Dias, G. Kiladis, F. Ahmed, S. W. Powell, E. Maloney, and M. Branson, 2020: Interactions between Moisture and Tropical Convection. Part I: The Coevolution of Moisture and Convection. *Journal of the Atmospheric Sciences*, **77**, 1783–1799, https://doi.org/10.1175/JAS-D-19-0225.1.

Zhang, F., 2005: Dynamics and Structure of Mesoscale Error Covariance of a Winter Cyclone Estimated through Short-Range Ensemble Forecasts. *Monthly Weather Review*, **133**, 2876–2893, https://doi.org/10.1175/MWR3009.1.

THIS PAGE INTENTIONALLY LEFT BLANK

INITIAL DISTRIBUTION LIST

1. Defense Technical Information Center
   Ft. Belvoir, Virginia

2. Dudley Knox Library
   Naval Postgraduate School
   Monterey, California